The Journal of Immunology

Intestinal CCL11 and Eosinophilic Inflammation Is Regulated by Myeloid Cell–Specific RelA/p65 in Mice

Amanda Waddell, Richard Ahrens, Yi-Ting Tsai, Joseph D. Sherrill, Lee A. Denson, Kris A. Steinbrecher and Simon P. Hogan

J Immunol 2013; 190:4773-4785; Prepublished online 5 April 2013;
doi: 10.4049/jimmunol.1200057
http://www.jimmunol.org/content/190/9/4773

The Journal of Immunology is published twice each month by
The American Association of Immunologists, Inc.,
1451 Rockville Pike, Suite 650, Rockville, MD 20852

Print ISSN: 0022-1767 Online ISSN: 1550-6606.

Intestinal CCL11 and Eosinophilic Inflammation Is Regulated by Myeloid Cell–Specific RelA/p65 in Mice

Amanda Waddell,* Richard Ahrens,* Yi-Ting Tsai,* Joseph D. Sherrill,* Lee A. Denson,† Kris A. Steinbrecher,† and Simon P. Hogan*

In inflammatory bowel diseases (IBDs), particularly ulcerative colitis, intestinal macrophages (MΦs), eosinophils, and the eosinophil-selective chemokine CCL11, have been associated with disease pathogenesis. MΦs, a source of CCL11, have been reported to be of a mixed classical (NF-κB–mediated) and alternatively activated (STAT-6–mediated) phenotype. The importance of NF-κB and STAT-6 pathways to the intestinal MΦ/CCL11 response and eosinophilic inflammation in the histopathology of experimental colitis is not yet understood. Our gene array analyses demonstrated elevated STAT-6– and NF-κB–dependent genes in pediatric ulcerative colitis colonic biopsies. Dextran sodium sulfate (DSS) exposure induced STAT-6 and NF-κB activation in mouse intestinal F4/80$^+$CD11b$^+$Ly6C^{hi} (inflammatory) MΦs. DSS-induced CCL11 expression, eosinophilic inflammation, and histopathology were attenuated in RelA/p65$^{\Delta mye}$ mice, but not in the absence of STAT-6. Deletion of p65 in myeloid cells did not affect inflammatory MΦ recruitment or alter apoptosis, but did attenuate LPS-induced cytokine production (IL-6) and *Ccl11* expression in purified F4/80$^+$CD11b$^+$Ly6C^{hi} inflammatory MΦs. Molecular and cellular analyses revealed a link between expression of calprotectin (*S100a8*/*S100a9*), *Ccl11* expression, and eosinophil numbers in the DSS-treated colon. In vitro studies of bone marrow–derived MΦs showed calprotectin-induced CCL11 production via a p65-dependent mechanism. Our results indicate that myeloid cell–specific NF-κB–dependent pathways play an unexpected role in CCL11 expression and maintenance of eosinophilic inflammation in experimental colitis. These data indicate that targeting myeloid cells and NF-κB–dependent pathways may be of therapeutic benefit for the treatment of eosinophilic inflammation and histopathology in IBD. ***The Journal of Immunology*****, 2013, 190: 4773–4785.**

Inflammatory bowel diseases (IBDs) are chronic, relapsing, remitting diseases of the gastrointestinal (GI) tract. Although the precise causes of IBD (ulcerative colitis [UC] and Crohn's disease) remain unclear, experimental and clinical studies indicate that activation of innate immune pathways trigger macrophage (MΦ) and dendritic cell activation, and subsequent cytokine production (IL-1β, IL-6, and TNF-α), driving IL-23/Th17 development and granulocyte (neutrophils and eosinophils) recruitment and activation leading to pathophysiological features of disease (1, 2). Monocytes/MΦs are elevated in colonic biopsy samples from patients with IBD, and these cells produce large amounts of proinflammatory cytokines (IL-6, TNF-α, and IL-23), as well as various chemokines, and retain respiratory burst activity (3–5). Corroborative experimental studies using chemical (dextran sodium sulfate [DSS]) and spontaneous models of IBD (IL-10$^{-/-}$) have identified a role for MΦs in augmentation and exacerbation of the intestinal inflammatory responses and pathogenesis in IBD (6–8).

Clinical and experimental evidence indicates a pathogenic role for eosinophils in both chemical (DSS) and spontaneous murine models (SAMP1/Yit and *Il10*$^{-/-}$) of colitis and in human IBD (9–12). Recent studies have reported that inflammatory MΦs express the eosinophil-specific chemokine CCL11 and have implicated this pathway in the regulation of eosinophilic inflammation in experimental colitis (13). Moreover, intestinal CD68$^+$ MΦs in colonic biopsy samples from pediatric patients wtih UC are positive for CCL11, and *CCL11* mRNA levels positively correlate with eosinophil numbers (9). The molecular regulation of CCL11 expression in MΦs is not yet fully understood; however, in vivo evidence from parasite infestation and rhinovirus models suggests that MΦ-driven eosinophilic inflammation is associated with an alternative MΦ activation phenotype (M2) and requires STAT-6 activation (14, 15). Consistent with this, CCL11 expression can be induced by IL-4 and IL-13; however, in vitro evidence in various cell lines indicates that cytokines including TNF-α, IL-9, and IL-17 can also stimulate CCL11 expression through activation of STAT-6–independent pathways including NF-κB, STAT-3, or MAPK-mediated signaling (16–19).

In this study, we demonstrate STAT-6 and NF-κB activation in colonic F4/80$^+$CD11b$^+$Ly6C^{hi} monocyte/MΦs during DSS-induced colitis. We show that DSS-induced F4/80$^+$CD11b$^+$Ly6C^{hi} monocyte/MΦ recruitment, CCL11 expression, and eosinophilic inflammation can occur in the absence of STAT-6. In contrast, loss of RelA/p65 in the myeloid lineage leads to decreased DSS-induced CCL11 secretion, eosinophil recruitment, IL-6 secretion, and histopathology. Purification of F4/80$^+$CD11b$^+$Ly6C^{hi} RelA/p65-

*Division of Allergy and Immunology, Cincinnati Children's Hospital Medical Center, Cincinnati, OH 45229; and †Division of Gastroenterology, Hepatology and Nutrition, Cincinnati Children's Hospital Medical Center, Cincinnati, OH 45229

Received for publication January 6, 2012. Accepted for publication February 20, 2013.

This work was supported by The Crohn's and Colitis Foundation of America Career Development Award (to S.P.H.), National Institutes of Health Grants R01 AI073553 and DK090119 (to S.P.H.), and an American Gastroenterological Association Foundation Graduate Student Research Fellowship Award (to A.W.).

Address correspondence and reprint requests to Dr. Simon P. Hogan or Dr. Kris A. Steinbrecher, Division of Allergy and Immunology, MLC 7028, Cincinnati Children's Hospital Medical Center, 3333 Burnet Avenue, Cincinnati, OH 45229 (S.P.H.) or Division of Gastroenterology, Hepatology and Nutrition, MLC 2010, Cincinnati Children's Hospital Medical Center, 3333 Burnet Avenue, Cincinnati, OH 45229 (K.A.S.). E-mail addresses: simon.hogan@cchmc.org (S.P.H.) or kris.steinbrecher@cchmc.org (K.A.S.)

The online version of this article contains supplemental material.

Abbreviations used in this article: BMDM, bone marrow–derived macrophage; DSS, dextran sodium sulfate; FSC, forward scatter; GI, gastrointestinal; HPF, high-power field; IBD, inflammatory bowel disease; IκB, inhibitor of κB; IKK, activation of inhibitor of IκB kinase; LysM, lysozyme M; MΦ, macrophage; MBP, major basic protein; qRT-PCR, quantitative real-time RT-PCR; RAGE, receptor for advanced glycation end product; SSC, side scatter; UC, ulcerative colitis; WT, wild-type.

deficient monocyte/MΦs from the colon of mice exposed to DSS revealed significantly reduced *Ccl11* expression. In vitro studies identify S100a8/S100a9-induced bone marrow–derived MΦ (BMDM)–derived CCL11 production via a p65-dependent mechanism. These studies demonstrate that MΦ-driven eosinophilic inflammation in experimental colitis is regulated by CCL11 and NF-κB–dependent pathways.

Materials and Methods

Mice

Male and female 6- to 8-wk-old strain-, age-, and weight-matched lysozyme M (LysM)$^{cre/cre}$RelA/p65$^{fl/fl}$ (RelA/p65$^{\Delta mye}$, C57BL/6/129/SvEv) and LysM$^{cre/cre}$RelA/p65$^{+/+}$ (wild-type [WT] line for RelA/p65$^{\Delta mye}$ mice) and STAT-6$^{-/-}$ (C57BL/6) (20) and WT C57BL/6 mice were used. All mice were housed under specific pathogen-free conditions and treated according to institutional guidelines.

DSS-induced colonic injury and histopathologic examination

DSS (MP Biomedicals, Santa Ana, CA, 40–45 kDa) was administered in the drinking water as a 2.5% (w/v) solution for up to 7 d. Disease monitoring and histopathologic changes in the colon were scored as previously described (9).

Western blot

BMDMs, spleen, or colonic epithelial lysates were run on 4–12% Bis-Tris gels and transferred to a nitrocellulose membrane (Invitrogen, Carlsbad, CA). The following Abs were used: rabbit anti–inhibitor of κB (IκB) kinase (anti–IKK-α), IκB-β, c-Rel, p105/p50 (Santa Cruz, Santa Cruz, CA), phosphoserine 536 RelA/p65, IκB-α (Cell Signaling, Danvers, MA), and total RelA/p65 (Rockland Immunochemicals, Gilbertsville, PA) followed by goat anti-rabbit peroxidase-conjugated Ab (Calbiochem, Darmstadt, Germany) and ECL-plus detection reagents (GE Healthcare, Buckinghamshire, U.K.). Rabbit anti-actin (Sigma, St. Louis, MO) was used as an internal loading control.

MΦ activation. BMDMs were obtained as described previously (21). The cells (1×10^6) were seeded onto 24-well plates and cultured overnight (37°C, 5% CO_2). The next day, cells were treated with LPS (1 μg/ml *P. gingivalis*; Invivogen, San Diego, CA), IL-4 (20 ng/ml), IFN-γ (1000 U/ml; PeproTech, Rocky Hill, NJ) for 24 h, and BMDMs and supernatants were assessed for active cleaved caspase-3 or cytokine production by ELISA. In some experiments, WT and RelA/p65$^{\Delta mye}$ BMDMs were stimulated with calprotectin (0.5 μg/ml; S100a8/S100a9 complex; Abcam, Cambridge, MA) for 24 h, and CCL11 levels were measured in the supernatants as described.

ELISA

CCL11, IL-6, IL-1β, and TNF-α levels were measured in the supernatants or lysates using the ELISA Duo-Set kit according to the manufacturer's instructions (R&D Systems, Minneapolis, MN). IL-12p40 was measured in the supernatants using the ELISA BD OptEIA kit according to the manufacturer's instructions (BD Biosciences, San Diego, CA).

Major basic protein staining

Eosinophil levels were quantified by anti-major basic protein (MBP) immunohistochemistry as previously described (22), and numbers are given as eosinophils per high-power field (HPF).

Punch biopsies

Colons were excised, flushed with PBS with gentamicin (20 μg/ml), and opened along a longitudinal axis. Thereafter, 3-mm^2 punch biopsies were excised and incubated for 24 h in 24-well plates with RPMI 1640 supplemented with 10% FCS and antibiotics. Supernatants were collected and kept at −80°C until assessed for cytokines/chemokines by ELISA.

Real-time RT-PCR analysis

Mouse *Hprt*, *RelA/p65*, *Ccl11*, *Retnla*, *Arg1*, *Cxcl2*, *Cxcl3*, *Cxcl10*, *Cxcl9*, *Il1b*, *Ccl22*, *Tnf*, *Il6*, *Nfkbia*, *Gapdh*, and *Il10* mRNA were quantified by quantitative real-time RT-PCR (qRT-PCR) as previously described (23). In brief, the RNA samples were subjected to reverse transcription analysis using SuperScript II reverse transcriptase (Invitrogen, Carlsbad, CA) according to the manufacturer's instructions and quantified using the iQ5 multicolor real-time PCR detection system (Bio-Rad Laboratories, Hercules, CA) with iQ5 software V2.0 and LightCycler FastStart DNA Master SYBR Green I. Gene expression was determined as relative expression on a linear curve based on a gel-extracted standard and was normalized to *Hprt* amplified from the same cDNA mix. Results were expressed as the gene of interest/*Hprt* ratio. *Nfkbia* expression was normalized to *Gapdh* and expressed as ΔΔCt.

Intestinal MΦ purification

MΦ populations from the colons were isolated as previously described (9). In brief, the colon segment of the GI tract was removed and flushed with 20 ml Ca^{2+}- and Mg^{2+}-free HBSS. The colon was cut longitudinally, placed in Ca^{2+}- and Mg^{2+}-free HBSS containing 10% FBS/5 mM EDTA/25 mM HEPES, and shaken vigorously at 37°C for 30 min. The tissue was cut into 1-cm segments and incubated in digestion buffer containing 2.4 mg/ml collagenase A (Roche Diagnostics, Indianapolis, IN) and 0.2 mg/ml DNase I (Roche Diagnostics) in RPMI 1640 for 45 min on a shaker at 37°C. After incubation, the cell aggregates were dissociated by filtering thorough a 19-gauge needle and 70-μm filter, and centrifuged at 1200 rpm for 20 min at 4°C. The supernatant was decanted and the cell pellet resuspended in 1% FBS/5 mM EDTA/PBS, and cells were incubated for 30 min with biotinylated rat anti-mouse CD11b (1 μg/1 $\times$ 10^6 cells; BD Pharmingen, San Jose, CA) at 4°C. Cells were subsequently incubated with anti-biotin microbeads (Miltenyi, Auburn, CA) for 15 min at 10°C and purified by LS MACS column by positive selection as described by the manufacturer. In brief, 1 ml cell suspension was added to the LS column, and the column was washed three times with 3 ml of 1% FBS/5 mM EDTA/PBS. CD11b$^+$ cells were removed from the column using a plunger. After washing, CD11b$^+$-selected cells were labeled with rat anti-mouse Ly6C-Alexa-647 (AbD Serotec, Raleigh, NC) and Streptavidin-PerCp (BD Pharmingen), and immediately sorted for CD11b and Ly6C using a FACSAria cell sorter (BD Biosciences, San Jose, CA). Purity of CD11b$^+$ Ly6C^{hi} cells was >95% as assessed by flow cytometry. RNA was isolated using the Qiagen RNeasy micro kit for cDNA synthesis and qRT-PCR analysis as described earlier.

FACS analysis

Single-cell suspensions were washed with FACS buffer (PBS/1% FBS) and incubated with combinations of the following Abs: PE anti-mouse F4/80 (clone CI:A3-1; Serotec, Raleigh, NC), PE-Cy7 anti-mouse CD11b (clone M1/70; BD Pharmingen), and AlexaFluor-647 anti-mouse Ly6C (clone ER-MP20; AbD Serotec, Raleigh, NC). For phosphoflow staining, cells were fixed with 2% formaldehyde/PBS for 10 min, permeabilized for 15 min with ice-cold methanol, and stained for 30 min at room temperature with AlexaFluor-647 anti-mouse p-RelA/p65 (polyclonal; Cell Signaling) or AlexaFluor-488 anti-mouse p-STAT-6 (polyclonal; Cell Signaling). For apoptosis analysis, cells were fixed and permeabilized using the BD cytofix/cytoperm kit followed by staining with the AlexaFluor-647 rabbit anti-active caspase-3 Ab (clone C92-605; BD Pharmingen). The following Abs were used as appropriate isotype controls: FITC rat IgG2a (clone B39-4; BD Pharmingen), PE rat IgG2a (clone 53-6.7; BD Pharmingen), PE-Cy7 rat IgG2b (clone DTA-1; BD Pharmingen), and AlexaFluor 647 rat IgG2a (clone R35-95; BD Pharmingen). Cells were analyzed on FACS-Calibur (BD Immunocytometry Systems, San Jose, CA), and analysis was performed using FlowJo software (Tree Star, Ashland, OR).

Microarray analysis

STAT-6– and NF-κB–regulated gene profiles were generated from colonic biopsy samples from pediatric UC and healthy patients as reported by Ahrens et al. (9). Gene expression profiles from DSS-treated mice (day 6: $n = 6$, day 0: $n = 5$) as reported by Fang et al. (24) were downloaded from the National Center for Biotechnology Information Gene Expression Omnibus database (accession no. GSE22307; http://www.ncbi.nlm.nih.gov/geo/query/acc.cgi?acc=GSE22307) and analyzed using GeneSpring GX software (version 11.5.1; Agilent Technologies). Data were baseline transformed to the median of all samples and compared against the DSS day 0 treatment group. Statistical analyses were performed using an unpaired *t* test and Benjamini–Hochberg false discovery rate. Genes showing significant differential expression ($p < 0.05$) with >2-fold change were assessed for correlation with *Ccl11* expression (Pearson $r > 0.075$), and hierarchical clustering was performed. Normalized log2-transformed expression levels of *Ear5*, *S100a8*, and *S100a9* from individual mice were plotted against *Ccl11* levels.

Statistical analysis

Data were analyzed by means of ANOVA, followed by the Tukey's or Dunnett's post hoc test or a two-tailed unpaired *t* test with GraphPad Prism

5 (San Diego, CA). Data are presented as the mean ± SE. The p values <0.05 were considered statistically significant.

Results

STAT-6– and NF-κB–induced genes are elevated in UC patients compared with normal patients

Recently, we demonstrated a relationship between intestinal $CD68^+$ MΦ-derived CCL11 and eosinophilic inflammation in pediatric UC patients (9). CCL11 expression is directly regulated by STAT-6– and NF-κB–mediated signaling through interactions with overlapping consensus DNA response elements within the CCL11 promoter (25, 26). To begin to distinguish the involvement of STAT-6– and NF-κB–mediated signaling in intestinal MΦ-derived CCL11 expression and eosinophilic inflammation, we examined for evidence of NF-κB– and STAT-6–dependent gene expression in a pediatric UC transcriptome generated from gene array analyses of colonic biopsy samples from pediatric UC and healthy patients (9). Analysis of the pediatric UC transcriptome revealed increased expression of STAT-6–regulated genes, including *IL13RA2* (16-fold), *SELP*, *SELE*, *CD40*, *COL1A1*, and *COL1A2* (Table I). The promoter regions of all these genes possess STAT-6 binding sites (27). STAT-6–dependent pathways are also involved in the induction of the alternatively activated MΦ phenotype (28), and we also observed increased expression of genes associated with alternative MΦ activation including *SERPINE1*, *CCL18*, and *SOCS1* (Table I). NF-κB–regulated genes were also significantly elevated in pediatric UC, including *CXCL5*, *IL8*, *CXCL2*, and *CXCL3*, which are all increased over 10-fold compared with healthy patients (Table II). These data demonstrate increased levels of both STAT-6– and NF-κB–regulated genes in pediatric UC.

CCL11 expression in IL-4–stimulated BMDMs is STAT-6–dependent

Previous in vitro and in vivo studies indicate a role for IL-4 in MΦ-derived STAT-6 activation and in the regulation of pulmonary eosinophilic inflammation (15). To begin to determine the requirement for IL-4–STAT-6 axis in CCL11 expression in MΦs, we examined CCL11 expression in IL-4–stimulated BMDMs generated in vitro. IL-4 stimulation of BMDMs induced STAT-6 activation (Supplemental Fig. 1A, 1B). STAT-6 activation was associated with increased *Ccl11* mRNA expression and significant CCL11 protein release (Supplemental Fig. 1D, 1E). Notably, IL-4 stimulation of MΦ induced alternative MΦ activation as demonstrated by increased expression of *Chi3l3*, *Arg1*, and *Retnla* (Supplemental Fig. 1C). The alternatively activated MΦ phenotype and *Ccl11* expression were dependent on STAT-6, as indicated by the loss of *Ccl11* and *Arg1* expression in STAT-$6^{-/-}$ BMDMs (Supplemental Fig. 1D, 1E). LPS stimulation of BMDMs did not induce *Ccl11* mRNA expression or significant protein release (results not shown). These data indicate that IL-4–induced, MΦ-derived CCL11 expression is STAT-6–dependent.

STAT-6 is not required for DSS-induced CCL11 expression or eosinophil recruitment

To assess the contribution of STAT-6 signaling to DSS-induced eosinophil recruitment and CCL11 expression, we performed phosphoflow analysis on isolated lamina propria cells from DSS-treated and vehicle (baseline)-treated mice. Levels of p-STAT-6 in the $F4/80^+CD11b^+Ly6C^{hi}$ colonic MΦs from DSS-treated WT mice were elevated compared with $F4/80^+CD11b^+Ly6C^{hi}$ MΦs from vehicle (baseline)-treated WT and DSS-treated STAT-$6^{-/-}$ mice (Fig. 1A; mean ± SD: p-STAT-6 mean fluorescence intensity WT control 6.03 ± 0.21; WT DSS 7.6 ± 0.4*; STAT-$6^{-/-}$ 6.5 ± 0.2; n = 3–7 samples/group; $*p < 0.05$). DSS treatment (6 d) of WT mice induced significant colitic disease characterized by cryptitis, epithelial ulceration, and pronounced inflammatory infiltrate, including significant eosinophilic inflammation (Fig. 1B–E). The absence of STAT-6 did not influence DSS-induced histopathology or eosinophil influx (Fig. 1B–E). Importantly, CCL11 levels were not different between WT and STAT-$6^{-/-}$ mice after DSS treatment (Fig. 1F). These data indicate that STAT-6 is not required for DSS-induced CCL11 expression, colonic eosinophil influx, and histopathology.

Myeloid cell–specific deletion of the RelA/p65 gene in mice (RelA/p65$^{\Delta mye}$)

We have previously reported increased classical and alternatively activated MΦ gene expression in purified $CCL11^+F4/80^+CD11b^+Ly6C^{hi}$ colonic MΦs from DSS-treated mice (13), suggesting activation of both STAT-6– and NF-κB–regulated pathways. Given our demonstration that CCL11 expression and colonic eosinophilic inflammation could occur in the absence of STAT-6, we next assessed the role of NF-κB. Phosphoflow analysis revealed increased levels of p-RelA/p65 in colonic $F4/80^+CD11b^+Ly6C^{hi}$ MΦs from DSS-treated mice compared with untreated mice (Fig. 2A). Consistent with this, quantitative RT-PCR analysis revealed a 10-fold increase in the mRNA levels of the NF-κB–dependent gene, *Nfkbia*, in this population compared with blood monocytes from DSS-treated mice (Fig. 2B). To delineate the requirement of NF-κB to the intestinal MΦ:CCL11:eosinophil pathway in colitis, we backcrossed RelA/$p65^{fl/fl}$ mice (29) onto the LysM-Cre mice (30) to specifically delete RelA/p65 in myeloid cells. To demonstrate the efficiency of the LysM-Cre–mediated deletion of RelA/p65, we assessed presence and activation (phosphorylation) of RelA/p65 in BMDMs (Fig. 2C). Western blot analyses revealed the loss of total RelA/p65 protein in RelA/$p65^{\Delta mye}$ BMDMs (Fig. 2C). Further, RelA/p65 activation was ablated in RelA/$p65^{\Delta mye}$

Table I. STAT-6–dependent gene expression in pediatric UC

Gene Name	Gene Symbol	UC versus NL (Fold Change)
IL-13 receptor, α2	*IL13RA2*	16.47
Selectin E	*SELE*	7.28
Collagen, type I α1	*COL1A1*	5.09
Chemokine (C-C motif) ligand 18	*CCL18*	4.77
Collagen, type I α2	*COL1A2*	4.36
Selectin P (granule membrane protein 140 kDa, Ag CD62)	*SELP*	3.37
Suppressor of cytokine signaling 1	*SOCS1*	2.49
Serpin peptidase inhibitor, clade E (nexin, plasminogen activator inhibitor type 1), membrane 1	*SERPINE1*	2.40
CD40 molecule, TNF receptor superfamily member 5	*CD40*	2.26

NL, Normal healthy patients.

Table II. NF-κB–dependent gene expression in pediatric UC

Gene Name	Gene Symbol	UC versus NL (Fold Change)
Chemokine (C-X-C motif) ligand 5	*CXCL5*	39.49
IL-8	*IL8*	21.24
Chemokine (C-X-C motif) ligand 2	*CXCL2*	11.68
Chemokine (C-X-C motif) ligand 3	*CXCL3*	10.35
Lipocalin 2 (oncogene 24p3)	*LCN2*	7.32
Selectin E	*SELE*	7.28
Ig heavy constant γ4	*IGHG4*	6.89
IL-1, β	*IL1B*	5.94
Chemokine (C-C motif) ligand 11	*CCL11*	5.87
PG-endoperoxidase synthase 2 (PG G/H synthase and cyclooxygenase)	*PTGS2*	5.59
Chemokine (C-X-C motif) ligand 10	*CXCL10*	4.35
IL-6	*IL6*	4.30
Secretory leukocyte peptidase inhibitor	*SLPI*	4.14
Matrix metallopeptidase 9 (gelatinase B, 92kDa gelatinase, 92kDa type IV collagenase)	*MMP9*	3.78
ICAM 1 (CD54)	*ICAM1*	3.64
Guanylate binding protein 1, IFN-inducible, 67 kDa	*GP1*	3.24
Chemokine (C-C motif) ligand 2	*CCL2*	3.01
Nucleotide-binding oligomerization domain-containing 2 protein	*NOD2*	2.96

NL, Normal healthy patients.

BMDMs after 1 h of LPS stimulation (Fig. 2C). RelA/p65 deletion was specific for the myeloid lineage, as we observed normal levels of total RelA/p65 in the spleen and colonic epithelium of RelA/p65$^{\Delta mye}$ mice (Fig. 2D).

To determine the effect of RelA/p65 deletion in myeloid cells on other components of the NF-κB signaling cascade, we assessed IKK-α, c-Rel, and p105 expression in BMDMs (Fig. 2E). We observed comparable levels of IKK-α, c-Rel, and p105 expression between WT and RelA/p65$^{\Delta mye}$ BMDMs after LPS stimulation (Fig. 2E). As expected, total levels of IκB-α and IκB-β were decreased in RelA/p65$^{\Delta mye}$ compared with WT BMDMs at time 0 (29, 31–33); however, these inhibitory proteins underwent comparable degradation after LPS stimulation, indicating that signaling components upstream of RelA/p65 remained intact (Fig. 2E). These data indicate selective RelA/p65 deletion in myeloid cells, and that this is independent of effects of other components of the NF-κB signaling pathway.

LPS-induced proinflammatory cytokine production in RelA/p65-deficient MΦs

To delineate the effect of RelA/p65 deficiency on MΦ proinflammatory cytokine production, we generated BMDMs from WT and RelA/p65$^{\Delta mye}$ mice, and examined responsiveness to LPS stimulation. BMDMs from RelA/p65$^{\Delta mye}$ mice develop normally, with comparable forward scatter (FSC), side scatter (SSC), F4/80, and CD11b expression compared with WT (data not shown). LPS-induced secretion of TNF-α, IL-6, IL-1β, and NO was significantly attenuated in RelA/p65$^{\Delta mye}$ BMDMs compared with WT (Fig. 2F). However, IL-12p40 secretion was similar between RelA/p65$^{\Delta mye}$ and WT BMDMs (Fig. 2F), which is consistent with functional c-Rel–dependent transcription (34). To assess NF-κB–independent pathway function in RelA/p65$^{\Delta mye}$ BMDMs, we measured type I IFN-induced chemokine (CXCL10) production in RelA/p65$^{\Delta mye}$ and WT BMDMs. Levels of type I IFN-induced STAT-1 phosphorylation and CXCL10 secretion were similar between RelA/p65$^{\Delta mye}$ and WT BMDMs (Supplemental Fig. 2A, 2B). Furthermore, assessment of active caspase-3 in IL-4 or IFN-γ + LPS-stimulated BMDMs revealed that deletion of RelA/p65 in MΦ does not alter MΦ apoptosis (Fig. 2G). These data indicate that RelA/p65$^{\Delta mye}$ MΦs have attenuated NF-κB–dependent proinflammatory cytokine responses; however, NF-κB–independent signaling such as type I IFN-induced STAT-1–dependent chemokine production remains intact.

DSS-induced colitis is attenuated in RelA/p65$^{\Delta mye}$ mice

To assess the requirement for myeloid expression of RelA/p65 in DSS-induced colonic injury, we exposed RelA/p65$^{\Delta mye}$ and aged- and strain-matched WT mice to 2.5% DSS for 6 d and examined colitic disease. RelA/p65 deletion in myeloid cells protected the mice from DSS-induced colonic injury (Fig. 3). DSS-induced weight loss, development of diarrhea, rectal bleeding, and colon shortening were significantly attenuated in RelA/p65$^{\Delta mye}$ mice compared with WT mice (Fig. 3A–C). Histological assessment of the colon revealed that the reduction in clinical symptoms of disease in RelA/p65$^{\Delta mye}$ mice was accompanied by a significant reduction in intestinal epithelial crypt loss, erosion, inflammatory infiltrate, and the proinflammatory cytokine IL-6 (Fig. 3D–F). Surprisingly, we observed no significant reduction in TNF-α or IL-1β in colonic punch biopsy samples between DSS-treated WT and RelA/p65$^{\Delta mye}$ mice (Fig. 3F). We observed no differences in intestinal immune and epithelial architecture between naive WT and RelA/p65$^{\Delta mye}$ mice, indicating no homeostatic effects of myeloid p65 deletion on intestinal function. Collectively, these studies identify that myeloid expression of RelA/p65 is required for DSS-induced increases in IL-6, intestinal inflammation, and colonic injury.

Attenuation of DSS-induced colitis is not due to decreased Ly6C^{hi} monocyte or neutrophil recruitment

Previous studies demonstrated that blockade of the recruitment of inflammatory MΦs to the colon via a CCR2-dependent pathway can attenuate DSS-induced colitis disease (13). We show that DSS exposure (5 d) induced a significant influx of F4/80^{+}CD11b^{+} Ly6C^{hi} monocytes in WT mice (Fig. 4A, 4B) (13). Importantly, loss of myeloid RelA/p65 did not dysregulate recruitment of Ly6C^{hi} monocytes to the colon at baseline or after DSS treatment (Fig. 4A, 4B). Similarly, we observed no reduction in neutrophil recruitment into the colon in RelA/p65$^{\Delta mye}$ mice (Fig. 4C, 4D). Peripheral blood levels of neutrophils and Ly6C^{hi} monocytes were also equivalent between WT and RelA/p65$^{\Delta mye}$ mice (Supplemental Fig. 3). These data indicate that myeloid trafficking to the colon during chronic inflammatory conditions does not require RelA/p65 signaling in myeloid cells.

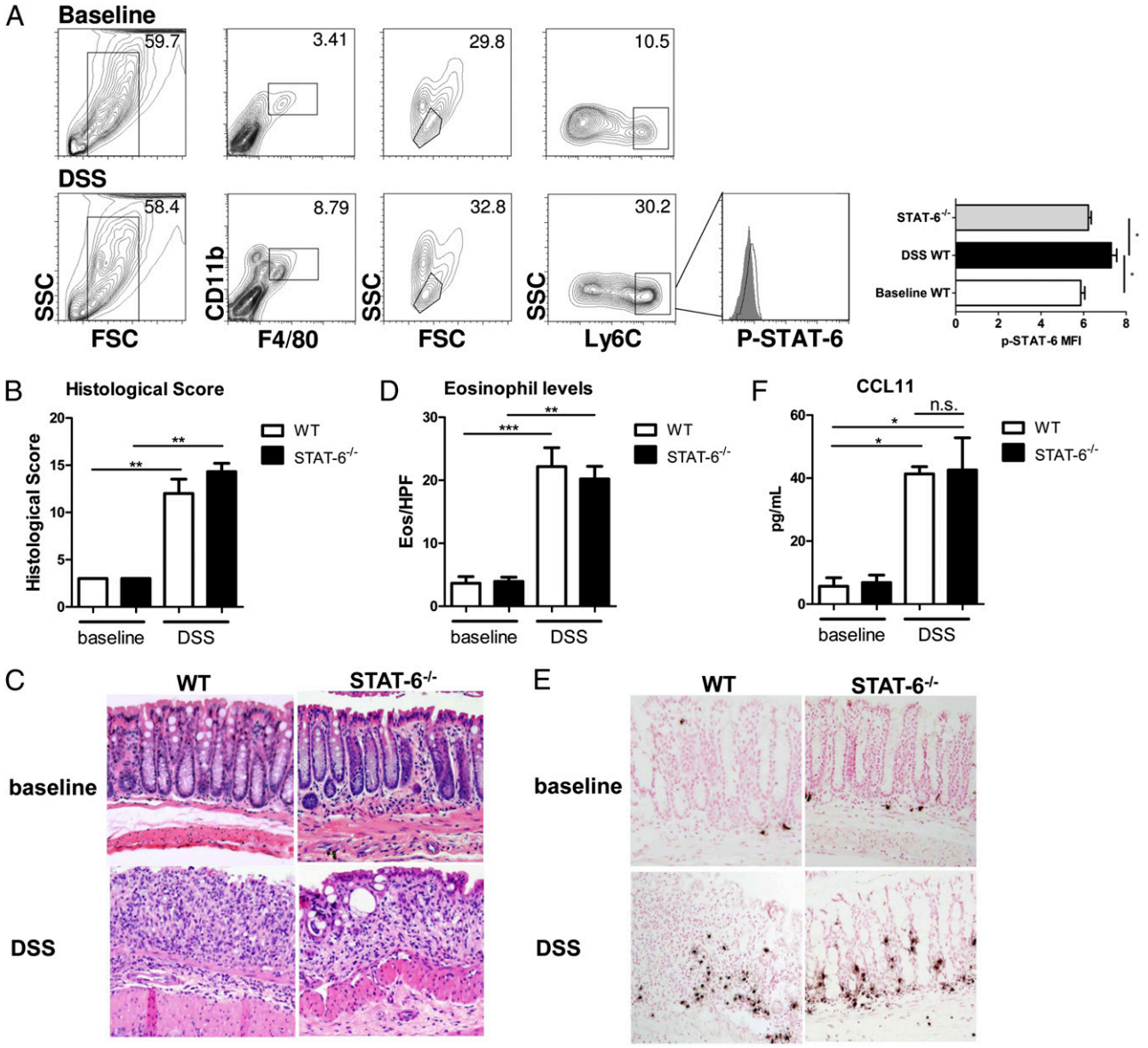

FIGURE 1. Eosinophil recruitment and CCL11 expression are STAT-6–independent in DSS-induced colitis. (**A**) Representative flow cytometry plots of F4/80^{+}CD11b^{+}Ly6C^{hi} colonic MΦs and representative histograms of p-STAT-6 expression in DSS-treated WT mice (open histograms) compared with STAT-6$^{-/-}$ mice (filled histograms) and mean fluorescence intensity of p-STAT-6. (**B**) Histological score. (**C**) Representative photomicrographs of H&E-stained colonic sections from baseline and DSS-treated mice (day 7, 2.5% DSS). (**D**) Eosinophil levels in the colon and (**E**) representative photomicrographs of anti-MBP–stained colonic sections from baseline and DSS-treated mice (day 7, 2.5% DSS). (C and E) Original magnification ×100. (**F**) CCL11 levels in punch biopsy supernatants from WT and STAT-6$^{-/-}$ mice at baseline and after 5 d of DSS. (A) Data represent the mean ± SEM of n = 3–7 mice/group from duplicate experiments. (B–F) Data represent the mean ± SEM of n = 5–6 mice/group. Data are representative of triplicate experiments. Significant differences ($*p < 0.05$, $**p < 0.01$, $***p < 0.001$) between groups. Eos, Eosinophils; n.s., Not significant.

Colonic eosinophilic inflammation is decreased in RelA/p65$^{\Delta mye}$ mice

Assessment of colonic eosinophil levels in DSS-treated RelA/p65$^{\Delta mye}$ mice revealed a significant decrease in induction of eosinophil levels compared with DSS-treated WT mice (Fig. 5A, 5B). The blunting of the DSS-induced increase in eosinophil number in RelA/p65$^{\Delta mye}$ mice was associated with a similar and significant lack of DSS-induced increase in CCL11 levels in colonic punch biopsies from DSS-treated RelA/p65$^{\Delta mye}$ mice (Fig. 5B). We have previously demonstrated that eosinophils are localized to the GI tract under homeostatic conditions, and that the recruitment of this cell population is regulated by CCL11 (35). Deletion of RelA/p65 in myeloid cells did not alter steady-state CCL11 and eosinophil levels, indicating that myeloid RelA/p65 does not regulate homeostatic CCL11 production or eosinophil recruitment. These data implicate the specificity of myeloid RelA/p65 in regulating the increase in CCL11 expression and colonic eosinophilic inflammation during colonic injury.

To directly determine whether the reduction in DSS-induced CCL11 in the colon of RelA/p65$^{\Delta mye}$ mice was a consequence of reduced CCL11 production from Ly6C^{hi} colonic MΦs, we used flow sorting to purify Ly6C^{hi} MΦs from the colon of DSS-treated mice using CD11b and Ly6C (Fig. 6A). PCR analyses revealed decreased *Ccl11* expression in DSS-treated RelA/p65$^{\Delta mye}$ Ly6C^{hi} colonic MΦs compared with WT (Fig. 6B). Importantly, the reduction in *Ccl11* expression in RelA/p65$^{\Delta mye}$ MΦs was not due to an inability to express CCL11, because IL-4 treatment induced

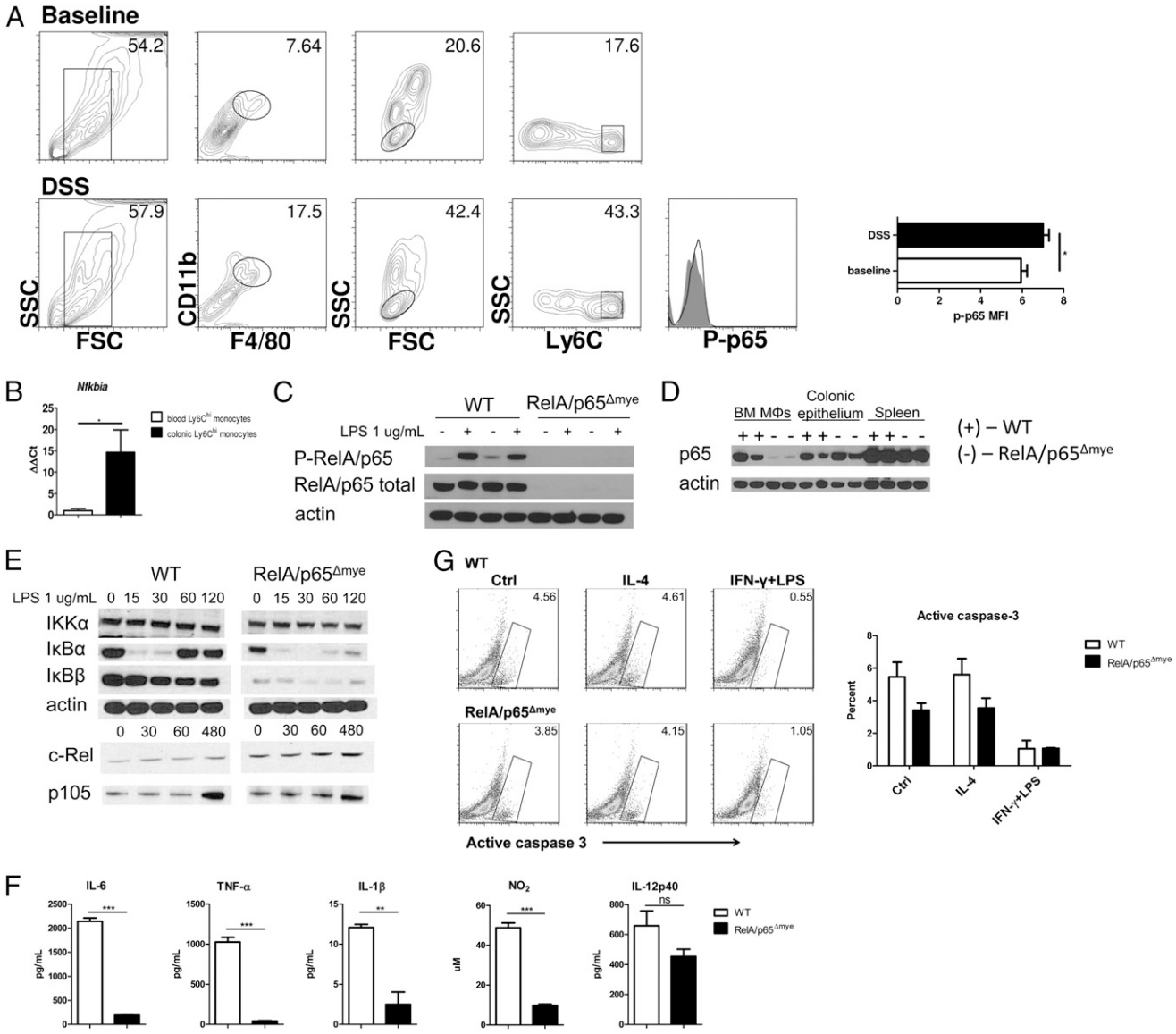

FIGURE 2. Specificity of RelA/p65 deletion in RelA/p65$^{\Delta mye}$ mice. (**A**) Representative flow cytometry plots and histograms of p-RelA/p65 expression in F4/80^{+}CD11b^{+}Ly6C^{hi} colonic MΦs from DSS-treated WT (open histograms) and untreated WT mice (filled histograms). (**B**) Quantification of *Nfkbia* expression from Ly6C^{hi} MΦs/monocytes sorted from the peripheral blood or colon of DSS-treated mice. Data represent the mean ± SEM of $n = 5$ mice/group. Representative Western blot analysis of WT (+) and RelA/p65$^{\Delta mye}$ (−) (**C**) BMDMs stimulated with 1 μg/ml LPS for 1 h; (**D**) colonic epithelium and spleen of total RelA/p65 and/or p-RelA/p65. (**E**) Representative Western blot analysis of IKK-α, IκB-α, IκB-β, c-Rel, p105, and actin expression in BMDMs stimulated with LPS for indicated times (minutes). (**F**) WT and RelA/p65$^{\Delta mye}$ BMDMs were stimulated for 24 h with vehicle or 1 μg/ml LPS, and levels of IL-6, TNF-α, IL-1β, NO_2, and IL-12p40 were measured in the supernatants. (**G**) Representative flow cytometry plots and graph of BMDMs stimulated for 24 h with control, IL-4, or IFN-γ + LPS and assessed for active caspase-3. (F and G) Data represent the mean ± SEM of $n = 3$ individual samples/group. (A, C, E–G) Data are representative of duplicate experiments. Significant differences ($*p < 0.05$, $**p < 0.01$, $***p < 0.001$) between groups. n.s., Not significant.

equivalent levels of *CCL11* expression in both WT and RelA/p65$^{\Delta mye}$ BMDMs (Supplemental Fig. 4).

We previously reported that Ly6C^{hi} colonic MΦs from DSS-treated mice had a mixed M1 and M2 proinflammatory phenotype (13). To assess the effect of myeloid cell–specific RelA/p65 deletion to this phenotype, we examined expression of M1 and M2 genes in purified Ly6C^{hi} colonic MΦs from WT and RelA/p65$^{\Delta mye}$ DSS-treated mice. Quantitative PCR analyses of RelA/p65 expression confirmed RelA/p65 deletion in purified Ly6C^{hi} colonic MΦs from RelA/p65$^{\Delta mye}$ DSS-treated mice (Ly6C^{hi} colonic MΦs RelA/*p65/hprt* ratio WT 1.41 ± 0.19 versus RelA/p65$^{\Delta mye}$ 0.37 ± 0.04; $n = 3$ purified F4/80^{+} CD11b^{+} Ly6C^{hi} colonic MΦ preparations per group; $p < 0.05$). *Il1b*, *Cxcl9* (M1), *Retnla*, *Il10*, and *Ccl22* (M2) gene expression was decreased in colonic Ly6C^{hi} MΦs from DSS-treated p65$^{\Delta mye}$ mice compared with DSS-treated WT mice, suggesting that these genes are positively regulated by RelA/p65 (Fig. 6B). *Cxcl10* and *Arg1* expression was also decreased, although not significantly. Surprisingly, *Tnf*, *Il6*, *Cxcl2*, and *Cxcl3* expression was not decreased in colonic Ly6C^{hi} MΦs from RelA/p65$^{\Delta mye}$ mice compared with WT mice (Fig. 6B), indicating that loss of RelA/p65 may not regulate their expression at the time examined.

Calprotectin–Receptor for advanced glycation end products involvement in MΦ-derived CCL11 production

To identify potential candidates involved in the stimulation of CCL11 expression and secretion in intestinal inflammatory MΦs in DSS-induced colitis, we reanalyzed microarray profiling analyses performed on the colon of control and DSS-treated C57BL/6 mice

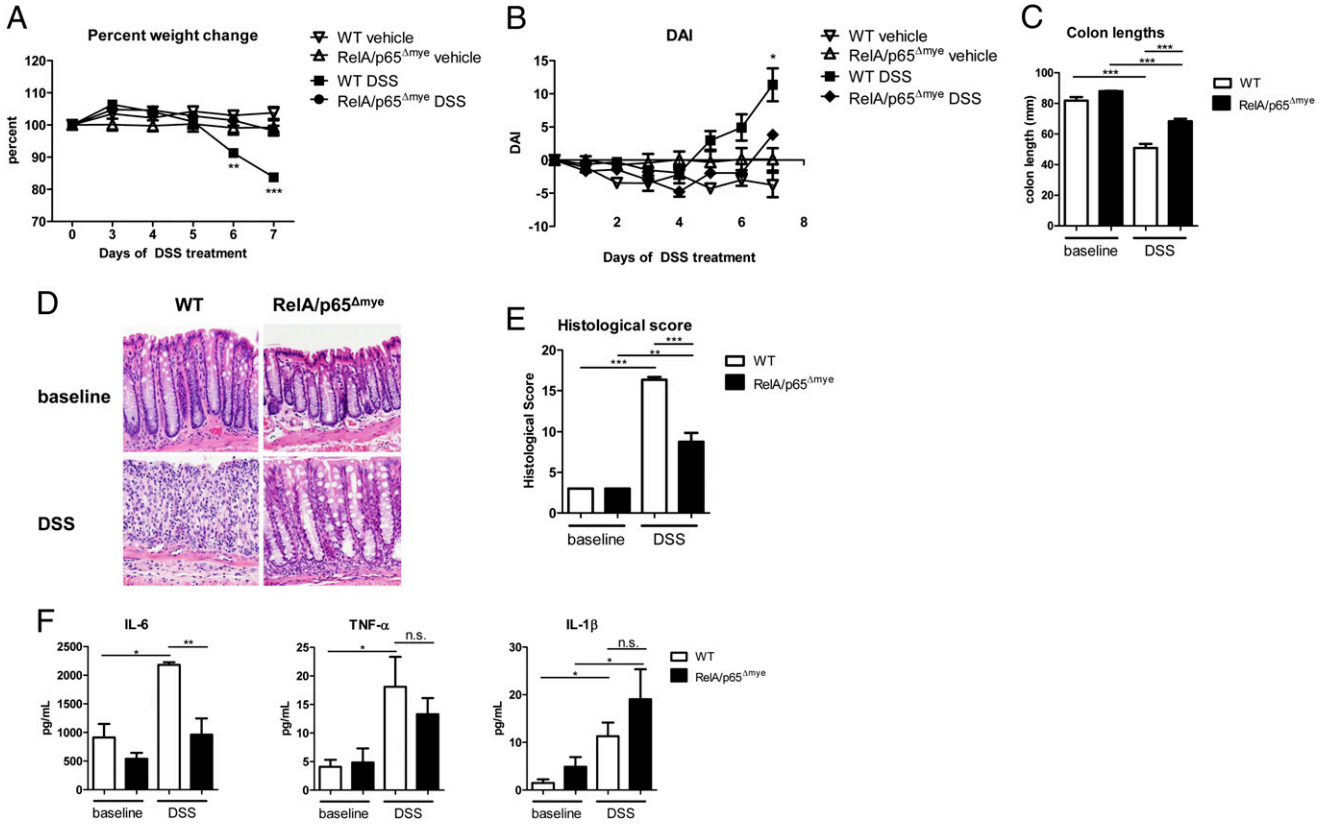

FIGURE 3. DSS-induced colitis is attenuated in RelA/p65$^{\Delta mye}$ mice. (**A**) Percent weight change and (**B**) disease activity index (DAI) of WT and RelA/p65$^{\Delta mye}$ mice after DSS exposure. (**C**) Colon lengths, (**D**) representative photomicrographs (original magnification ×100), and (**E**) quantitative histological score of H&E-stained colonic sections from of WT and p65$^{\Delta mye}$ mice after 7 d of DSS exposure. (**F**) Cytokine profile of colonic punch biopsy samples from WT and RelA/p65$^{\Delta mye}$ mice after DSS exposure. Data represent the mean ± SEM of n = 3–5 mice/group. Data are representative of triplicate (A–E) and duplicate (F) experiments. Significant differences (*$p < 0.05$, **$p < 0.01$, ***$p < 0.001$) compared with WT vehicle or as indicated. n.s., Not significant.

(data accessible at National Center for Biotechnology Information Gene Expression Omnibus database [24], accession no. GSE22307). These array data are of the colon of C57BL/6 mice after 0 and 6 d of DSS (3%), and changes in gene expression have been validated by qRT-PCR with $r^2 = 0.925122$ (24). We compared gene expression at days 0 and 6 as we have previously demonstrated maximal inflammatory MΦ recruitment into the colon on day 6 of DSS exposure (9). Three percent DSS exposure induced the upregulation of 1008 genes and downregulation 173 genes (results not shown). Consistent with the previous gene array analysis comparing gene expression between day 0 versus day 6 of DSS exposure, we revealed increased expression of inflammatory genes, including *Il6*, *Cxcl2*, *Cxcl1*, *Il33*, and *Il1b* (Fig. 7A and results not shown) (24). Assessment of *Ccl11* and eosinophil-specific genes (e.g., *Ear5*, eosinophil-associated, RNase A family, member 5) revealed significant elevated levels of *Ccl11* and *Ear5* mRNA (3.2- and 2.7-fold increase, respectively). Correlative analyses demonstrated a positive correlation between *Ccl11* and *Ear5* mRNA expression ($r = 0.82$; $p < 0.001$; Fig. 7C). These data are consistent with our previous studies in C57BL/6 demonstrating a direct relationship between CCL11 and eosinophils (9, 13). The top DSS-induced genes (day 0 versus day 6 of DSS exposure) that correlated with *Ccl11* expression were *Saa3* (47.6-fold increase), *Mmp3* (45.4-fold increase), and the S100 proteins, *S100a8* (46.1-fold increase) and *S100a9* (43.3-fold increase; Fig. 7B). Notably, *S100a8* and *S100a9* were the highest upregulated genes that possessed the strongest positive correlation with *Ccl11* mRNA expression (*S100a8*: $r = 0.68$, $p < 0.03$; *S100a9*: $r = 0.70$, $p < 0.02$; Fig. 7B, 7C). These studies revealed a relationship between *S100a8* and *S100a9*, colonic CCL11 expression, and eosinophilic inflammation in DSS-induced colitis. To confirm these observations, we assessed *S100a8* and *S100A9* mRNA expression and eosinophil numbers in the colon after 0, 3, and 7 d of DSS exposure (Fig. 7D). We demonstrate a positive correlation between *S100a8* and *S100a9* mRNA expression and eosinophil numbers/HPF in the colon during DSS exposure (Fig. 7D; $p < 0.01$). The S100a8/S100a9 (calprotectin) receptor is not fully delineated; however, there is evidence that the 35-kDa multiligand receptor for advanced glycation end products (RAGE) acts as the primary receptor for calprotectin (36, 37). Flow cytometry analyses revealed expression of the calprotectin receptor RAGE on Ly6C^{hi} colonic MΦs after 6 d of DSS exposure. Notably, the Ly6C^{hi} colonic MΦs and not the resident Ly6C^{low} colonic MΦs expressed RAGE (Fig. 7E). To assess whether calprotectin induced CCL11 expression in MΦs, we assessed S100a8/S100a9 stimulation of BMDMs. First, we show that BMDMs express the RAGE (Fig. 7F). Stimulation of BMDMs with heterodimeric calprotectin complex induced CCL11 secretion. Notably, the calprotectin response was dependent on NF-κB signaling as the calprotectin-induced CCL11 secretion was ablated in RelA/p65-deficient BMDMs (Fig. 7G). These studies indicate that calprotectin (S100a8/S100a9) induces CCL11 secretion in MΦs via an NF-κB–dependent pathway.

Discussion

In this study, we investigated the contribution of STAT-6 and NF-κB RelA/p65 in myeloid cells in the regulation of colonic eosinophilic inflammation and histopathology of DSS-induced colitis. Expression of both NF-κB– and STAT-6–dependent genes are increased in pediatric UC colonic biopsies. We report that NF-κB

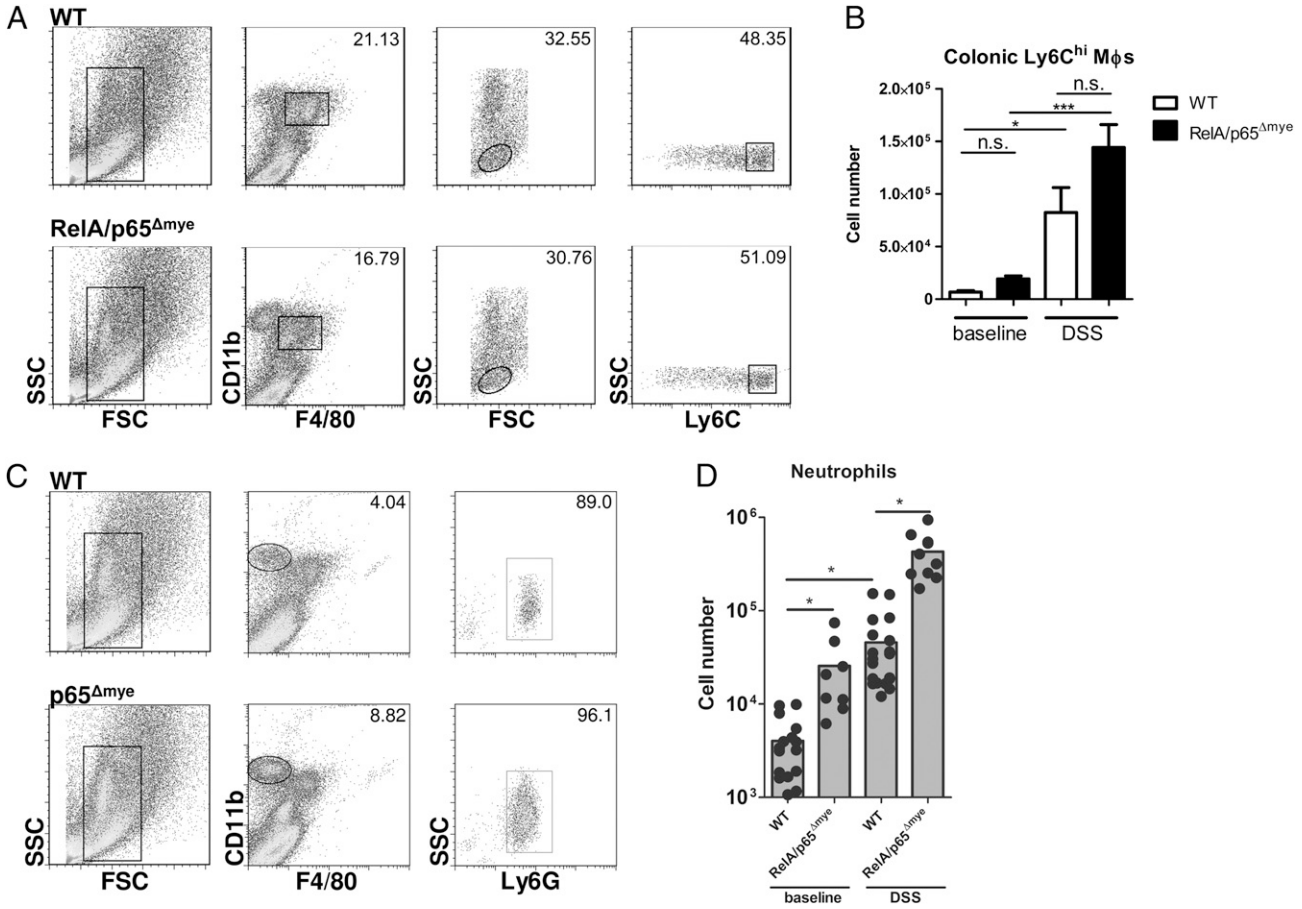

FIGURE 4. Colonic recruitment of myeloid cells is not impaired in RelA/p65$^{\Delta mye}$ mice. (**A**) Representative flow cytometry plots and (**B**) quantification of the F4/80^{+}CD11b^{+}Ly6C^{hi} MΦ populations from the colon of WT and RelA/p65$^{\Delta mye}$ mice after 5 d of vehicle (baseline) or DSS exposure. MΦs were initially gated by SSC versus FSC followed by F4/80^{+}, CD11b^{+}, and Ly6C^{hi}. (**C**) Representative flow cytometry plots and (**D**) quantification of the F4/80^{-}CD11b^{hi} neutrophil population from the colon of WT and RelA/p65$^{\Delta mye}$ mice after 5 d of vehicle (baseline) or DSS exposure. Neutrophils were initially gated by SSC versus FSC followed by F4/80^{-} and CD11b^{hi}. (B and D) Data represent the mean ± SEM of n = 5–6 mice/group and are representative of duplicate experiments. Closed circles indicate individual mice. Significant differences ($*p < 0.05$, $***p < 0.001$) between groups. n.s., Not significant.

and STAT-6 are activated in colonic Ly6C^{hi} MΦs during DSS-induced colitis in mice. We show that loss of STAT-6 does not alter susceptibility to colitic disease, whereas loss of RelA/p65 in myeloid cells leads to decreased susceptibility to DSS-induced colitis. Notably, attenuated DSS-induced clinical symptoms and histopathology in RelA/p65$^{\Delta mye}$ mice was associated with decreased induction of the proinflammatory cytokine IL-6, CCL11 expression, and eosinophil recruitment, and was not due to reduced recruitment of myeloid cells. We show that the reduced CCL11 levels in DSS-treated RelA/p65$^{\Delta mye}$ mice were linked with attenuated *Ccl11* expression in Ly6C^{hi} colonic MΦs. We identify a positive correlation between calprotectin (*S100A8* and *S100A9*) mRNA expression and colonic eosinophil numbers and that calprotectin stimulation of BMDMs leads to RelA/p65-dependent CCL11 secretion.

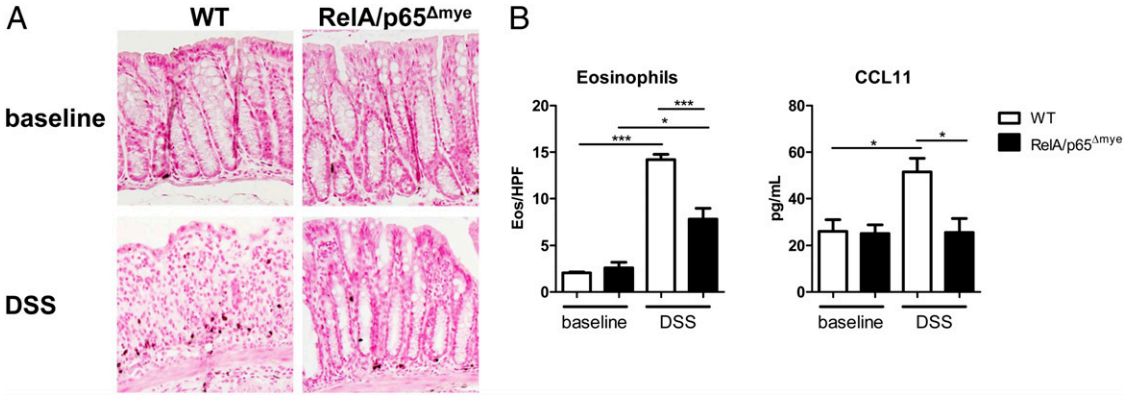

FIGURE 5. Lack of induction of CCL11 and eosinophils in RelA/p65$^{\Delta mye}$ mice during DSS-induced colitis. (**A**) Representative photomicrographs of anti-MBP–stained colonic sections from baseline and DSS-treated mice (day 6, 2.5%) and colonic eosinophil levels in the colon. Original magnification ×100. (**B**) CCL11 levels in punch biopsy supernatants from WT and RelA/p65$^{\Delta mye}$ mice in vehicle- (baseline) and DSS-treated mice (day 5, 2.5%). Data indicate the mean ± SEM of n = 6–8 mice/group from triplicate experiments. Significant differences ($*p < 0.05$, $***p < 0.001$) between groups. Eos, Eosinophils.

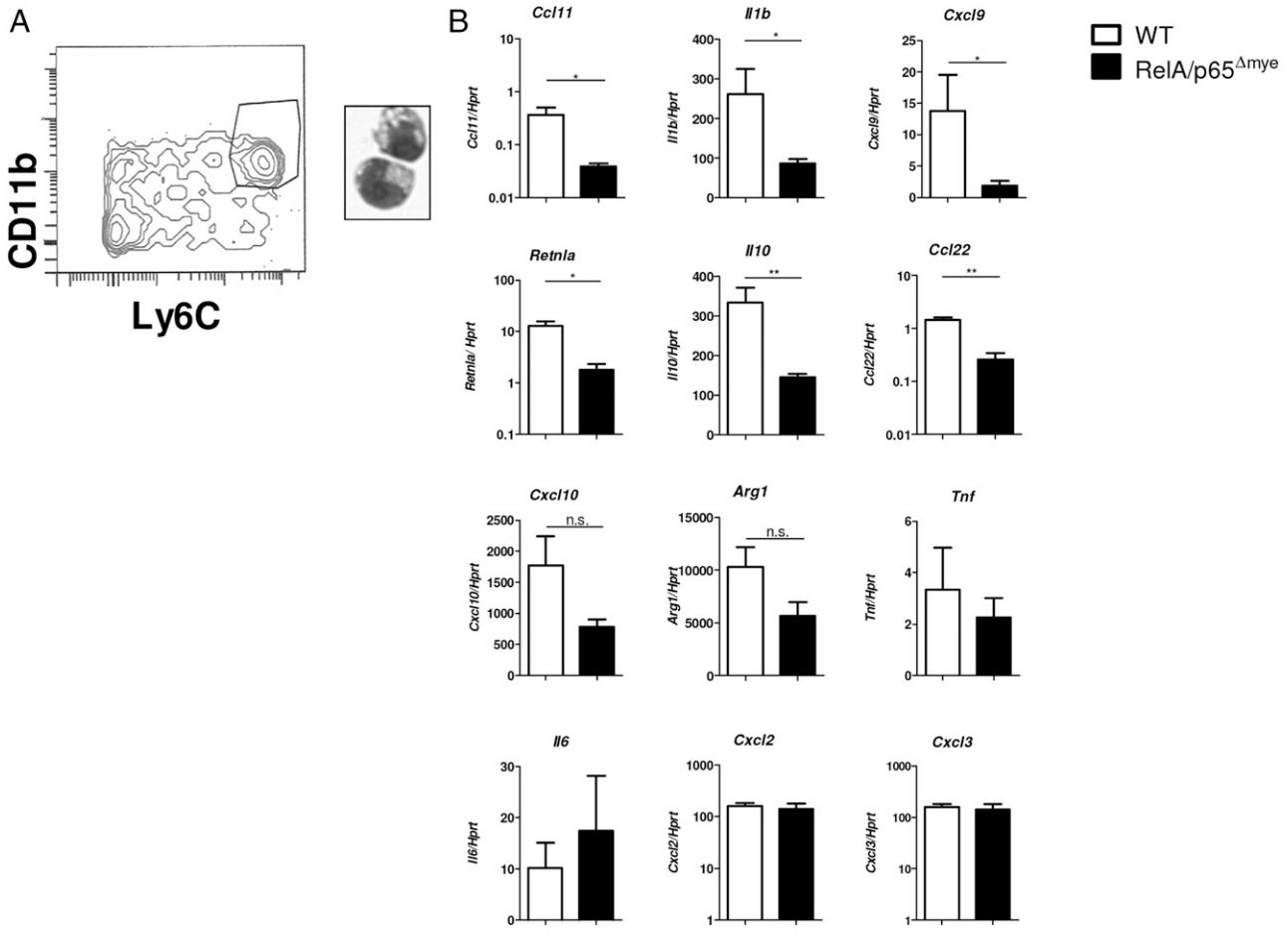

FIGURE 6. Phenotype of Ly6C^{hi} colonic MΦs in WT versus RelA/p65$^{\Delta mye}$ mice during DSS-induced colonic injury. (**A**) Representative flow cytometry plot of WT CD11b^{+}Ly6C^{hi} colonic MΦs flow sorted on day 5 of DSS treatment. (**B**) Gene expression was analyzed by qRT-PCR. Three to four mice were pooled per sample from DSS-treated WT and RelA/p65$^{\Delta mye}$ mice (3–4 samples/group). Data represent the mean ± SEM. Data are representative of duplicate experiments. Significant differences (*$p < 0.05$, **$p < 0.01$) between groups. n.s., Not significant.

Collectively, these data indicate that myeloid RelA/p65 plays a central role in the proinflammatory cytokine response and CCL11:eosinophil axis in experimental colitis.

Previous in vivo studies in models of heart transplant rejection (38), pulmonary hypertension (39), rhinovirus (15), and helminth infection (14) have identified a role for MΦs in eosinophil recruitment. The majority of these studies show that MΦ-mediated eosinophil recruitment is associated with M2 MΦ alternate activation and CCL11 expression. Consistent with this finding, we show that IL-4 stimulation of BMDMs induces the M2 MΦ phenotype and CCL11 expression, and that this pathway is dependent on STAT-6. However, our in vivo analyses revealed that CCL11-dependent eosinophil recruitment can occur in the absence of STAT-6 signaling. Previous studies have reported STAT-6–independent CCL11 expression in airway epithelial cells, and that this was mediated by TNF-α–induced NF-κB binding to the *CCL11* promoter (25). Consistent with this, in a mouse model of allergic lung inflammation, NF-κB inhibition by NF-κB decoy oligodeoxynucleotides or by genetic approaches (transgenic CC10-IκB-α–superrepressor mice) attenuated lung inflammation and reduced CCL11 expression (40, 41). Although these studies identified an interaction between NF-κB–regulated pathways and CCL11 expression, they did not elucidate the role of NF-κB in specific cell types. Our study indicates that at least in DSS-induced colitis, Ly6C^{hi} colonic MΦ-derived RelA/p65 regulates CCL11 levels and eosinophilic inflammation; however, it still remains to be determined whether RelA/p65 directly binds to the *CCL11* promoter in colonic MΦs.

Clinical and experimental evidence identify an important contribution by MΦs through the production of proinflammatory cytokines, including TNF-α, IL-6, IL-1β, and IL-23 in the exacerbation of the chronic inflammatory response in IBD and experimental colitis (3, 13, 42, 43). We show that myeloid deletion of RelA/p65 signaling attenuated DSS-induced colitic disease and IL-6 levels in punch biopsy samples. However, we did not observe reduced secreted TNF-α levels between WT and RelA/p65$^{\Delta mye}$ mice. This was somewhat surprising because we identified an important role for RelA/p65 in LPS-induced MΦ-derived TNF-α expression in vitro. Assessment of total TNF-α expression (secreted and nonsecreted) by analyzing whole colonic lysates did reveal a decrease in TNF-α expression in RelA/p65$^{\Delta mye}$ mice compared with WT (results not shown). These potential conflicting observations may be attributed to the fact that MΦs may not be the primary source of TNF-α in the colon during DSS-induced colitis, as human intestinal epithelial cells, mast cells, and NK cells are also able to produce TNF-α (44, 45). Gene expression analysis of purified Ly6C^{hi} colonic MΦs from RelA/p65$^{\Delta mye}$ mice revealed that decreased susceptibility to colitic disease was associated with lower levels of a number of proinflammatory genes: *Il1b*, *Retnla*, *Cxcl9*, *Cxcl10*, *Arg1*, and *Ccl22*. CXCL9 and CXCL10 are both increased in IBD patients (46, 47), and inhibition of CXCL10 protected mice from DSS-induced colitis (48).

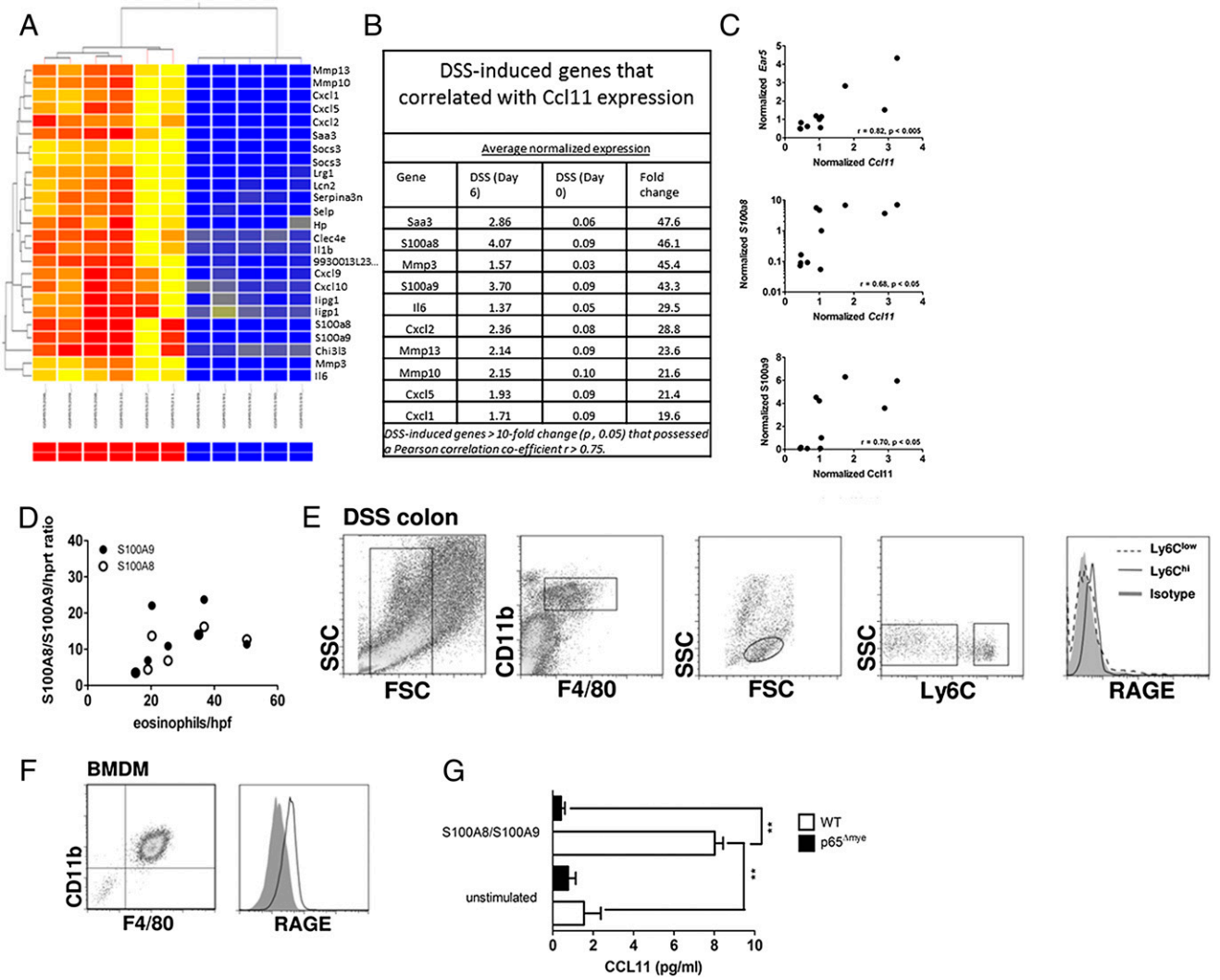

FIGURE 7. Relationship between eosinophil-specific gene (*Ear5*), *Ccl11*, and Calprotectin (S100a8 and S100a9) expression in DSS-induced colitis. (**A**) Heat map showing the clustering of the top 25 differentially expressed genes after DSS-induced colitis (day 6 versus day 0, $p < 0.05$). (**B**) Top 10 differentially expressed genes after DSS-induced colitis (day 6 versus day 0, $p < 0.05$, fold change > 10) that correlated with *Ccl11* expression ($r > 0.75$). (**C**) Pearson product-moment correlation between normalized microarray expression values of *Ear5*, *S100a8*, and *S100a9* are plotted against *Ccl11* from individual animals. (**D**) Pearson product-moment correlation between *S100a8* and *S100a9*/Hprt ratio and eosinophils/HPF in the colon of WT C57BL6 mice on days 3, 5, and 7 after DSS exposure. (**E**) Representative flow plots of RAGE expression on (E) colonic F4/80$^+$CD11b$^+$Ly6C^{hi} monocytes/MΦ from DSS-treated mice (day 6) and (**F**) BMDM. (**G**) CCL11 levels in supernatants from WT and RelA/p65$^{\Delta mye}$ BMDM after 24-h stimulation with S100a8/S100a9 complex. (G) Data represent the mean ± SEM. Data are representative of duplicate experiments. Significant differences (**$p < 0.01$) between groups.

Furthermore, we have previously demonstrated that *Retnla*$^{-/-}$ mice had decreased susceptibility to DSS-induced colitis (21). *Ccl22* expression is increased in DSS-induced colitis and in the sera of UC and Crohn's disease patients, but its role in IBD is not known (49, 50). These data indicate that MΦs express many proinflammatory genes that may contribute to chronic intestinal inflammatory phenotypes and disease pathology.

Previous studies have demonstrated that DSS exposure stimulates neutrophil recruitment into the colon (51). Consistent with this, we observed a significant increase in the level of neutrophil infiltration into the colon after DSS exposure in both the WT (~12-fold) and RelA/p65$^{\Delta mye}$ (16-fold) mice. However, neutrophil levels in the colon of RelA/p65$^{\Delta mye}$ mice were greater than that observed in WT mice under both steady-state and after DSS exposure. There are a number of potential explanations for this observation. First, LysM^{cre}-mediated deletion of RelA/p65 is occurring in neutrophils and may effect neutrophil migration or apoptosis. RelA/p65 has been implicated in neutrophil apoptosis, and the initial description of the LysM^{cre} transgene revealed efficient LysM^{cre} expression and deletion of floxed targeted genes in neutrophils (30). Alternatively, increased levels of neutrophils in the RelA/p65$^{\Delta mye}$ mice may be attributed to decreased MΦ function and activity. Interestingly, deletion of MΦs in the LysM^{cre} c-FLIP$^{fl/fl}$ mice was associated with heightened neutrophilia (52). The authors demonstrated that the increased neutrophil levels was a consequence of heightened G-CSF and IL-1β, and not necessarily caused by c-FLIP deletion in neutrophils as neutralization of G-CSF and IL-1β (anti–G-CSF and IL-1R antagonist) reduced neutrophil levels back to baseline levels (52). Notably, we observed increased levels of IL-1β in the colon of RelA/p65$^{\Delta mye}$ mice after DSS treatment. The molecular basis for the heightened neutrophil response in the RelA/p65$^{\Delta mye}$ mice is under current investigation.

Experimental analyses suggest that NF-κB activity in different cell populations has differential roles in the maintenance of tissue homeostasis versus proinflammatory function (29, 53–58). For example, intestinal epithelial cell–specific deletion of IKK complex proteins or RelA/p65 increased susceptibility to infection, spontaneous inflammation, and DSS-induced colitis (29, 53, 59).

Conversely, transgenic overexpression of constitutively active IKK-β in intestinal epithelial cells drives intestinal inflammation and cancer (54). In contrast, whole animal or hematopoietic cell inhibition of NF-κB using genetic, antisense oligonucleotides, or small-molecule inhibitors ameliorated mucosal inflammation (55–58). We demonstrate that selective deletion of RelA/p65 in myeloid cells attenuates intestinal inflammation and colitic disease, further emphasizing tissue-specific functions for the NF-κB pathway in homeostasis versus inflammation.

Previous studies using inducible IKK-β knockout mice (Mx^{cre}/$IKK\text{-}\beta^{fl/fl}$) have demonstrated that TNF-α–dependent apoptosis in the absence of IKK-β results in increased IL-1β protein secretion and granulocytosis (60), and LPS-induced apoptosis in myeloid cells was increased in $IKK\text{-}\beta^{\Delta mye}$ BMDMs (61). Notably, a number of IKK-β substrates and effector pathways are NF-κB–independent and control proliferation, apoptosis, and cytokine production. IKK-β regulation of MAPK activation, mTOR signaling, expression of autophagy genes, and proteins that regulate cell division and death such as Aurora A, p53, and FOXO3a can occur independently of NF-κB activity (62). Thus, one may predict a partial phenotypic overlap between mice lacking myeloid RelA/p65 and those deficient in myeloid IKK-β. Consistent with this, we show that genetic deletion of RelA/p65 in myeloid cells did not affect peripheral MΦ or neutrophil numbers, indicating that RelA/p65 is not required for MΦ and neutrophil antiapoptosis. Furthermore, apoptosis was not substantially increased after LPS stimulation of $RelA/p65^{\Delta mye}$ BMDMs compared with WT. Collectively, these data indicate the presence of RelA/p65-independent IKK-β substrates and activity in the regulation of myeloid cell function.

NF-κB activity is tightly controlled by interactions with the NF-κB inhibitory proteins, IκB-α and IκB-β. We show that the absence of RelA/p65 in BMDMs reduced baseline levels of the IκB-α and IκB-β. Notably, the levels of IκB-β were significantly lower than that observed of IκB-α, suggesting preferential loss of IκB-β. Deletion of RelA/p65 in mouse embryonic fibroblasts and primary liver fetal cells has also been associated with reduced levels of IκB-α and IκB-β, and similar to our data, the reduction in IκB-β levels was greater than that of IκB-α (32). The preferential reduction in IκB-β is attributed to the greater importance of RelA/p65 in stabilizing IκB-β protein, and protecting IκB-β from 26S proteasome degradation (32).

We have previously demonstrated in pediatric UC that CCL11 is derived from both intestinal epithelial cells and $CD68^+$ myeloid cells (9). In contrast, in the murine system using in situ hybridization and immunofluorescence technologies, we show that CCL11 is derived from mononuclear cells, primarily $Ly6C^{hi}$ colonic MΦs (13). One possible explanation for this discrepancy is that the peak DSS-induced colonic eosinophilic inflammation (day 6) is observed in the presence of a pronounced colonic epithelial ulceration and shedding, and that this may eliminate any intestinal epithelial CCL11 signal. Assessment of murine colonic intestinal epithelial cells from mice treated with DSS for 4 d revealed a positive CCL11 signal suggesting that murine intestinal epithelial cells may express CCL11 (results not shown). However, bone marrow chimera experiments demonstrate that $Ly6C^{hi}$ colonic MΦs are sufficient to drive CCL11-dependent colonic eosinophilic inflammation (13).

One limitation of these analyses is that deletion of RelA/p65 in myeloid cells using the $LysM^{Cre}$ system leads to deletion of RelA/p65 in all monocyte/MΦ subpopulations including the $Ly6C^{low}$ colonic tissue resident MΦs and the $Ly6C^{hi}$ inflammatory MΦs. Thus, we cannot exclude the contribution of RelA/p65 signaling in $Ly6C^{low}$ colonic tissue resident MΦs to DSS-induced CCL11 expression and eosinophilic inflammation. However, we have previously demonstrated that DSS exposure does not alter the levels of resident $Ly6C^{low}$ colonic tissue MΦs (13), and that loss of the $Ly6C^{hi}$ inflammatory MΦs and not resident $Ly6C^{low}$ colonic tissue MΦs in the colon was associated with reduced CCL11 levels and eosinophilic inflammation (13), indicating that $Ly6C^{hi}$ inflammatory MΦs are likely the MΦ subpopulation responsible for CCL11 and eosinophilic inflammation in the colon during epithelial injury.

Bioinformatics analyses and in vitro studies on BMDMs reveal that calprotectin, the S100a8/S100a9 heterodimeric complex, may be the stimulus for MΦ-derived CCL11 secretion. Indeed, we show that BMDM and inflammatory-recruited $Ly6C^{hi}$ colonic MΦs express the calprotectin receptor RAGE, and that the expression of S100a9 and S100a8 in the colon of DSS-treated mice positively correlated with eosinophil numbers. S100A8 and S100A9 are members of the S100 protein family and the EF-hand protein superfamily (63), and are intracellular proteins that exist mainly as a heterodimer (termed calprotectin). Recent work indicates that S100a8 and S100a9 also possess extracellular functions and regulate leukocyte migration, cytokine expression, and innate immune activity (64–66). The receptor for S100A8/S100A9 (calprotectin) is not fully delineated; however, there is evidence that the 35-kDa multiligand receptor RAGE acts as the primary receptor for calprotectin (36, 37). Previous experimental evidence indicates that calprotectin induces NF-κB activation in $RAGE^+$ cells (37, 67), and that calprotectin-induced myeloid-derived cell migration and accumulation was RAGE- and NF-κB–dependent (68). We show that calprotectin induced BMDM-derived CCL11 secretion, and that this was dependent on NF-κB signaling. There is significant clinical evidence suggesting calprotectin and RAGE involvement in IBD. Fecal calprotectin levels are elevated in pediatric UC and Crohn's disease, and levels positively correlate with disease severity and mucosal inflammation (69, 70). Notably, fecal calprotectin levels are one of the most accurate measurements for the presence of active mucosal inflammation and likelihood of IBD relapse (71). Furthermore, calprotectin is a stronger predictive marker of relapse in UC than in Crohn's disease because patients under clinical remission who recorded a higher initial concentration of fecal calprotectin (>150 μg/g) are 2 and 14 times more likely to relapse in Crohn's disease and UC, respectively (72). RAGE mRNA and protein levels are also increased in colonic samples of Crohn's disease patients, and the functional RAGE -374T/A polymorphism has been linked with Crohn's disease (73). RAGE is expressed on many hemapoietic (MΦs, neutrophils, dendritic cells, and B and T lymphocytes) and nonhemapoietic cell populations (74), and small interfering RNA (si-S100A9) knockdown of S100A9 reduced DSS-induced granulocyte infiltration and colitis disease activity (75).

Recent clinical evidence suggesting a central function for MΦs in the exacerbation of the chronic inflammatory response and manifestations of IBD has led to intense focus on the identification of MΦ-mediated intestinal inflammatory cascades. We have highlighted the importance of recently recruited $Ly6C^{hi}$ colonic MΦs in eosinophil recruitment and CCL11 expression. We now demonstrate that this is regulated by myeloid expression of RelA/p65 and is surprisingly STAT-6–independent. These studies provide significant rationale for the assessment of RelA/p65 activation in the expression of monocyte/MΦ-derived CCL11 in human IBD and further highlight the importance of targeting of the monocyte/MΦ:RelA/p65 pathway as a therapeutic modality for the treatment and prevention of IBD.

Acknowledgments

We thank Drs. Patricia Fulkerson and DeBroski Herbert and members of the Division of Allergy and Immunology and Gastroenterology, Hepatology,

and Nutrition, Cincinnati Children's Hospital Medical Center for critical review of the manuscript and insightful conversations. We thank Jamie Lee and Nancy Lee for the generous provision of anti-MBP Ab. We also thank Shawna Hottinger for editorial assistance and manuscript preparation.

Disclosures

S.P.H. is a consultant for Immune Pharmaceuticals. The other authors have no financial conflicts of interest.

References

1. Heinsbroek, S. E., and S. Gordon. 2009. The role of macrophages in inflammatory bowel diseases. *Expert Rev. Mol. Med.* 11: e14.
2. Xavier, R. J., and D. K. Podolsky. 2007. Unravelling the pathogenesis of inflammatory bowel disease. *Nature* 448: 427–434.
3. Kamada, N., T. Hisamatsu, S. Okamoto, H. Chinen, T. Kobayashi, T. Sato, A. Sakuraba, M. T. Kitazume, A. Sugita, K. Koganei, et al. 2008. Unique CD14 intestinal macrophages contribute to the pathogenesis of Crohn disease via IL-23/IFN-gamma axis. *J. Clin. Invest.* 118: 2269–2280.
4. Rugtveit, J., G. Haraldsen, A. K. Høgåsen, A. Bakka, P. Brandtzaeg, and H. Scott. 1995. Respiratory burst of intestinal macrophages in inflammatory bowel disease is mainly caused by CD14+L1+ monocyte derived cells. *Gut* 37: 367–373.
5. Reinecker, H. C., M. Steffen, T. Witthoeft, I. Pflueger, S. Schreiber, R. P. MacDermott, and A. Raedler. 1993. Enhanced secretion of tumour necrosis factor-alpha, IL-6, and IL-1 beta by isolated lamina propria mononuclear cells from patients with ulcerative colitis and Crohn's disease. *Clin. Exp. Immunol.* 94: 174–181.
6. Ghia, J. E., F. Galeazzi, D. C. Ford, C. M. Hogaboam, B. A. Vallance, and S. Collins. 2008. Role of M-CSF-dependent macrophages in colitis is driven by the nature of the inflammatory stimulus. *Am. J. Physiol. Gastrointest. Liver Physiol.* 294: G770–G777.
7. Watanabe, N., K. Ikuta, K. Okazaki, H. Nakase, Y. Tabata, M. Matsuura, H. Tamaki, C. Kawanami, T. Honjo, and T. Chiba. 2003. Elimination of local macrophages in intestine prevents chronic colitis in interleukin-10-deficient mice. *Dig. Dis. Sci.* 48: 408–414.
8. Takeda, K., B. E. Clausen, T. Kaisho, T. Tsujimura, N. Terada, I. Förster, and S. Akira. 1999. Enhanced Th1 activity and development of chronic enterocolitis in mice devoid of Stat3 in macrophages and neutrophils. *Immunity* 10: 39–49.
9. Ahrens, R., A. Waddell, L. Seidu, C. Blanchard, R. Carey, E. Forbes, M. Lampinen, T. Wilson, E. Cohen, K. Stringer, et al. 2008. Intestinal macrophage/epithelial cell-derived CCL11/eotaxin-1 mediates eosinophil recruitment and function in pediatric ulcerative colitis. *J. Immunol.* 181: 7390–7399.
10. Woodruff, S. A., J. C. Masterson, S. Fillon, Z. D. Robinson, and G. T. Furuta. 2011. Role of eosinophils in inflammatory bowel and gastrointestinal diseases. *J. Pediatr. Gastroenterol. Nutr.* 52: 650–661.
11. Takedatsu, H., K. Mitsuyama, S. Matsumoto, K. Handa, A. Suzuki, H. Takedatsu, H. Funabashi, Y. Okabe, T. Hara, A. Toyonaga, and M. Sata. 2004. Interleukin-5 participates in the pathogenesis of ileitis in SAMP1/Yit mice. *Eur. J. Immunol.* 34: 1561–1569.
12. Specht, S., S. Arriens, and A. Hoerauf. 2006. Induction of chronic colitis in IL-10 deficient mice requires IL-4. *Microbes Infect.* 8: 694–703.
13. Waddell, A., R. Ahrens, K. Steinbrecher, B. Donovan, M. E. Rothenberg, A. Munitz, and S. P. Hogan. 2011. Colonic eosinophilic inflammation in experimental colitis is mediated by Ly6C(high) CCR2(+) inflammatory monocyte/macrophage-derived CCL11. *J. Immunol.* 186: 5993–6003.
14. Voehringer, D., N. van Rooijen, and R. M. Locksley. 2007. Eosinophils develop in distinct stages and are recruited to peripheral sites by alternatively activated macrophages. *J. Leukoc. Biol.* 81: 1434–1444.
15. Nagarkar, D. R., E. R. Bowman, D. Schneider, Q. Wang, J. Shim, Y. Zhao, M. J. Linn, C. L. McHenry, B. Gosangi, J. K. Bentley, et al. 2010. Rhinovirus infection of allergen-sensitized and -challenged mice induces eotaxin release from functionally polarized macrophages. *J. Immunol.* 185: 2525–2535.
16. Yamasaki, A., A. Saleh, L. Koussih, S. Muro, A. J. Halayko, and A. S. Gounni. 2010. IL-9 induces CCL11 expression via STAT3 signalling in human airway smooth muscle cells. *PLoS ONE* 5: e9178.
17. Saleh, A., L. Shan, A. J. Halayko, S. Kung, and A. S. Gounni. 2009. Critical role for STAT3 in IL-17A-mediated CCL11 expression in human airway smooth muscle cells. *J. Immunol.* 182: 3357–3365.
18. Rahman, M. S., A. Yamasaki, J. Yang, L. Shan, A. J. Halayko, and A. S. Gounni. 2006. IL-17A induces eotaxin-1/CC chemokine ligand 11 expression in human airway smooth muscle cells: role of MAPK (Erk1/2, JNK, and p38) pathways. *J. Immunol.* 177: 4064–4071.
19. Matsukura, S., M. Odaka, M. Kurokawa, H. Kuga, T. Homma, H. Takeuchi, K. Notomi, F. Kokubu, M. Kawaguchi, R. P. Schleimer, et al. 2010. Transforming growth factor-beta stimulates the expression of eotaxin/CC chemokine ligand 11 and its promoter activity through binding site for nuclear factor-kappaB in airway smooth muscle cells. *Clin. Exp. Allergy* 40: 763–771.
20. Urban, J. F., Jr., N. Noben-Trauth, D. D. Donaldson, K. B. Madden, S. C. Morris, M. Collins, and F. D. Finkelman. 1998. IL-13, IL-4Ralpha, and Stat6 are required for the expulsion of the gastrointestinal nematode parasite *Nippostrongylus brasiliensis*. *Immunity* 8: 255–264.
21. Munitz, A., A. Waddell, L. Seidu, E. T. Cole, R. Ahrens, S. P. Hogan, and M. E. Rothenberg. 2008. Resistin-like molecule alpha enhances myeloid cell activation and promotes colitis. *J. Allergy Clin. Immunol.* 122: 1200–1207, e1.
22. Forbes, E., T. Murase, M. Yang, K. I. Matthaei, J. J. Lee, N. A. Lee, P. S. Foster, and S. P. Hogan. 2004. Immunopathogenesis of experimental ulcerative colitis is mediated by eosinophil peroxidase. *J. Immunol.* 172: 5664–5675.
23. Blanchard, C., N. Wang, K. F. Stringer, A. Mishra, P. C. Fulkerson, J. P. Abonia, S. C. Jameson, C. Kirby, M. R. Konikoff, M. H. Collins, et al. 2006. Eotaxin-3 and a uniquely conserved gene-expression profile in eosinophilic esophagitis. *J. Clin. Invest.* 116: 536–547.
24. Fang, K., M. Bruce, C. B. Pattillo, S. Zhang, R. Stone, II, J. Clifford, and C. G. Kevil. 2011. Temporal genomewide expression profiling of DSS colitis reveals novel inflammatory and angiogenesis genes similar to ulcerative colitis. *Physiol. Genomics* 43: 43–56.
25. Matsukura, S., C. Stellato, J. R. Plitt, C. Bickel, K. Miura, S. N. Georas, V. Casolaro, and R. P. Schleimer. 1999. Activation of eotaxin gene transcription by NF-kappa B and STAT6 in human airway epithelial cells. *J. Immunol.* 163: 6876–6883.
26. Hoeck, J., and M. Woisetschläger. 2001. STAT6 mediates eotaxin-1 expression in IL-4 or TNF-alpha-induced fibroblasts. *J. Immunol.* 166: 4507–4515.
27. Hebenstreit, D., G. Wirnsberger, J. Horejs-Hoeck, and A. Duschl. 2006. Signaling mechanisms, interaction partners, and target genes of STAT6. *Cytokine Growth Factor Rev.* 17: 173–188.
28. Biswas, S. K., and A. Mantovani. 2010. Macrophage plasticity and interaction with lymphocyte subsets: cancer as a paradigm. *Nat. Immunol.* 11: 889–896.
29. Steinbrecher, K. A., E. Harmel-Laws, R. Sitcheran, and A. S. Baldwin. 2008. Loss of epithelial RelA results in deregulated intestinal proliferative/apoptotic homeostasis and susceptibility to inflammation. *J. Immunol.* 180: 2588–2599.
30. Clausen, B. E., C. Burkhardt, W. Reith, R. Renkawitz, and I. Förster. 1999. Conditional gene targeting in macrophages and granulocytes using LysMcre mice. *Transgenic Res.* 8: 265–277.
31. Scott, M. L., T. Fujita, H. C. Liou, G. P. Nolan, and D. Baltimore. 1993. The p65 subunit of NF-kappa B regulates I kappa B by two distinct mechanisms. *Genes Dev.* 7(7A): 1266–1276.
32. Hertlein, E., J. Wang, K. J. Ladner, N. Bakkar, and D. C. Guttridge. 2005. RelA/p65 regulation of IkappaBbeta. *Mol. Cell. Biol.* 25: 4956–4968.
33. Sun, S. C., P. A. Ganchi, D. W. Ballard, and W. C. Greene. 1993. NF-kappa B controls expression of inhibitor I kappa B alpha: evidence for an inducible autoregulatory pathway. *Science* 259: 1912–1915.
34. Sanjabi, S., A. Hoffmann, H. C. Liou, D. Baltimore, and S. T. Smale. 2000. Selective requirement for c-Rel during IL-12 P40 gene induction in macrophages. *Proc. Natl. Acad. Sci. USA* 97: 12705–12710.
35. Mishra, A., S. P. Hogan, J. J. Lee, P. S. Foster, and M. E. Rothenberg. 1999. Fundamental signals that regulate eosinophil homing to the gastrointestinal tract. *J. Clin. Invest.* 103: 1719–1727.
36. Gebhardt, C., A. Riehl, M. Durchdewald, J. Németh, G. Fürstenberger, K. Müller-Decker, A. Enk, B. Arnold, A. Bierhaus, P. P. Nawroth, et al. 2008. RAGE signaling sustains inflammation and promotes tumor development. *J. Exp. Med.* 205: 275–285.
37. Turovskaya, O., D. Foell, P. Sinha, T. Vogl, R. Newlin, J. Nayak, M. Nguyen, A. Olsson, P. P. Nawroth, A. Bierhaus, et al. 2008. RAGE, carboxylated glycans and S100A8/A9 play essential roles in colitis-associated carcinogenesis. *Carcinogenesis* 29: 2035–2043.
38. Zweifel, M., K. Matozan, C. Dahinden, T. Schaffner, and P. Mohacsi. 2010. Eotaxin/CCL11 levels correlate with myocardial fibrosis and mast cell density in native and transplanted rat hearts. *Transplant. Proc.* 42: 2763–2766.
39. Weng, M., D. M. Baron, K. D. Bloch, A. D. Luster, J. J. Lee, and B. D. Medoff. 2011. Eosinophils are necessary for pulmonary arterial remodeling in a mouse model of eosinophilic inflammation-induced pulmonary hypertension. *Am. J. Physiol. Lung Cell. Mol. Physiol.* 301: L927–L936.
40. Poynter, M. E., R. Cloots, T. van Woerkom, K. J. Butnor, P. Vacek, D. J. Taatjes, C. G. Irvin, and Y. M. Janssen-Heininger. 2004. NF-kappa B activation in airways modulates allergic inflammation but not hyperresponsiveness. *J. Immunol.* 173: 7003–7009.
41. Desmet, C., P. Gosset, B. Pajak, D. Cataldo, M. Bentires-Alj, P. Lekeux, and F. Bureau. 2004. Selective blockade of NF-kappa B activity in airway immune cells inhibits the effector phase of experimental asthma. *J. Immunol.* 173: 5766–5775.
42. Schenk, M., A. Bouchon, F. Seibold, and C. Mueller. 2007. TREM-1—expressing intestinal macrophages crucially amplify chronic inflammation in experimental colitis and inflammatory bowel diseases. *J. Clin. Invest.* 117: 3097–3106.
43. Platt, A. M., C. C. Bain, Y. Bordon, D. P. Sester, and A. M. Mowat. 2010. An independent subset of TLR expressing CCR2-dependent macrophages promotes colonic inflammation. *J. Immunol.* 184: 6843–6854.
44. Bischoff, S. C., A. Lorentz, S. Schwengberg, G. Weier, R. Raab, and M. P. Manns. 1999. Mast cells are an important cellular source of tumour necrosis factor alpha in human intestinal tissue. *Gut* 44: 643–652.
45. Jung, H. C., L. Eckmann, S. K. Yang, A. Panja, J. Fierer, E. Morzycka-Wroblewska, and M. F. Kagnoff. 1995. A distinct array of proinflammatory cytokines is expressed in human colon epithelial cells in response to bacterial invasion. *J. Clin. Invest.* 95: 55–65.
46. Egesten, A., M. Eliasson, A. I. Olin, J. S. Erjefält, A. Bjartell, P. Sangfelt, and M. Carlson. 2007. The proinflammatory CXC-chemokines GRO-alpha/CXCL1 and MIG/CXCL9 are concomitantly expressed in ulcerative colitis and decrease during treatment with topical corticosteroids. *Int. J. Colorectal Dis.* 22: 1421–1427.

47. Noguchi, A., K. Watanabe, S. Narumi, H. Yamagami, Y. Fujiwara, K. Higuchi, N. Oshitani, and T. Arakawa. 2007. The production of interferon-gamma-inducible protein 10 by granulocytes and monocytes is associated with ulcerative colitis disease activity. *J. Gastroenterol.* 42: 947–956.
48. Sasaki, S., H. Yoneyama, K. Suzuki, H. Suriki, T. Aiba, S. Watanabe, Y. Kawauchi, H. Kawachi, F. Shimizu, K. Matsushima, et al. 2002. Blockade of CXCL10 protects mice from acute colitis and enhances crypt cell survival. *Eur. J. Immunol.* 32: 3197–3205.
49. Melgar, S., M. Drmotova, E. Rehnström, L. Jansson, and E. Michaëlsson. 2006. Local production of chemokines and prostaglandin E2 in the acute, chronic and recovery phase of murine experimental colitis. *Cytokine* 35: 275–283.
50. Jugde, F., M. Alizadeh, C. Boissier, D. Chantry, L. Siproudhis, S. Corbinais, E. Quelvennec, F. Dyard, J. P. Campion, M. Gosselin, et al. 2001. Quantitation of chemokines (MDC, TARC) expression in mucosa from Crohn's disease and ulcerative colitis. *Eur. Cytokine Netw.* 12: 468–477.
51. Qualls, J. E., A. M. Kaplan, N. van Rooijen, and D. A. Cohen. 2006. Suppression of experimental colitis by intestinal mononuclear phagocytes. *J. Leukoc. Biol.* 80: 802–815.
52. Gordy, C., H. Pua, G. D. Sempowski, and Y. W. He. 2011. Regulation of steady-state neutrophil homeostasis by macrophages. *Blood* 117: 618–629.
53. Zaph, C., A. E. Troy, B. C. Taylor, L. D. Berman-Booty, K. J. Guild, Y. Du, E. A. Yost, A. D. Gruber, M. J. May, F. R. Greten, et al. 2007. Epithelial-cell-intrinsic IKK-beta expression regulates intestinal immune homeostasis. *Nature* 446: 552–556.
54. Vlantis, K., A. Wullaert, Y. Sasaki, M. Schmidt-Supprian, K. Rajewsky, T. Roskams, and M. Pasparakis. 2011. Constitutive IKK2 activation in intestinal epithelial cells induces intestinal tumors in mice. *J. Clin. Invest.* 121: 2781–2793.
55. Greten, F. R., L. Eckmann, T. F. Greten, J. M. Park, Z. W. Li, L. J. Egan, M. F. Kagnoff, and M. Karin. 2004. IKKbeta links inflammation and tumorigenesis in a mouse model of colitis-associated cancer. *Cell* 118: 285–296.
56. Murano, M., K. Maemura, I. Hirata, K. Toshina, T. Nishikawa, N. Hamamoto, S. Sasaki, O. Saitoh, and K. Katsu. 2000. Therapeutic effect of intracolonically administered nuclear factor kappa B (p65) antisense oligonucleotide on mouse dextran sulphate sodium (DSS)-induced colitis. *Clin. Exp. Immunol.* 120: 51–58.
57. Davé, S. H., J. S. Tilstra, K. Matsuoka, F. Li, T. Karrasch, J. K. Uno, A. R. Sepulveda, C. Jobin, A. S. Baldwin, P. D. Robbins, and S. E. Plevy. 2007. Amelioration of chronic murine colitis by peptide-mediated transduction of the IkappaB kinase inhibitor NEMO binding domain peptide. *J. Immunol.* 179: 7852–7859.
58. Eckmann, L., T. Nebelsiek, A. A. Fingerle, S. M. Dann, J. Mages, R. Lang, S. Robine, M. F. Kagnoff, R. M. Schmid, M. Karin, et al. 2008. Opposing functions of IKKbeta during acute and chronic intestinal inflammation. *Proc. Natl. Acad. Sci. USA* 105: 15058–15063.
59. Nenci, A., C. Becker, A. Wullaert, R. Gareus, G. van Loo, S. Danese, M. Huth, A. Nikolaev, C. Neufert, B. Madison, et al. 2007. Epithelial NEMO links innate immunity to chronic intestinal inflammation. *Nature* 446: 557–561.
60. Mankan, A. K., O. Canli, S. Schwitalla, P. Ziegler, J. Tschopp, T. Korn, and F. R. Greten. 2011. TNF-alpha-dependent loss of IKKbeta-deficient myeloid progenitors triggers a cytokine loop culminating in granulocytosis. *Proc. Natl. Acad. Sci. USA* 108: 6567–6572.
61. Park, J. M., F. R. Greten, A. Wong, R. J. Westrick, J. S. Arthur, K. Otsu, A. Hoffmann, M. Montminy, and M. Karin. 2005. Signaling pathways and genes that inhibit pathogen-induced macrophage apoptosis—CREB and NF-kappaB as key regulators. *Immunity* 23: 319–329.
62. Oeckinghaus, A., M. S. Hayden, and S. Ghosh. 2011. Crosstalk in NF-κB signaling pathways. *Nat. Immunol.* 12: 695–708.
63. Marenholz, I., C. W. Heizmann, and G. Fritz. 2004. S100 proteins in mouse and man: from evolution to function and pathology (including an update of the nomenclature). *Biochem. Biophys. Res. Commun.* 322: 1111–1122.
64. Sunahori, K., M. Yamamura, J. Yamana, K. Takasugi, M. Kawashima, H. Yamamoto, W. J. Chazin, Y. Nakatani, S. Yui, and H. Makino. 2006. The S100A8/A9 heterodimer amplifies proinflammatory cytokine production by macrophages via activation of nuclear factor kappa B and p38 mitogen-activated protein kinase in rheumatoid arthritis. *Arthritis Res. Ther.* 8: R69.
65. Kerkhoff, C., I. Eue, and C. Sorg. 1999. The regulatory role of MRP8 (S100A8) and MRP14 (S100A9) in the transendothelial migration of human leukocytes. *Pathobiology* 67: 230–232.
66. Kerkhoff, C., M. Klempt, and C. Sorg. 1998. Novel insights into structure and function of MRP8 (S100A8) and MRP14 (S100A9). *Biochim. Biophys. Acta* 1448: 200–211.
67. Boyd, J. H., B. Kan, H. Roberts, Y. Wang, and K. R. Walley. 2008. S100A8 and S100A9 mediate endotoxin-induced cardiomyocyte dysfunction via the receptor for advanced glycation end products. *Circ. Res.* 102: 1239–1246.
68. Sinha, P., C. Okoro, D. Foell, H. H. Freeze, S. Ostrand-Rosenberg, and G. Srikrishna. 2008. Proinflammatory S100 proteins regulate the accumulation of myeloid-derived suppressor cells. *J. Immunol.* 181: 4666–4675.
69. Aomatsu, T., A. Yoden, K. Matsumoto, E. Kimura, K. Inoue, A. Andoh, and H. Tamai. 2011. Fecal calprotectin is a useful marker for disease activity in pediatric patients with inflammatory bowel disease. *Dig. Dis. Sci.* 56: 2372–2377.
70. Lewis, J. D. 2011. The utility of biomarkers in the diagnosis and therapy of inflammatory bowel disease. *Gastroenterology* 140: 1817–1826.e2.
71. Canani, R. B., L. T. de Horatio, G. Terrin, M. T. Romano, E. Miele, A. Staiano, L. Rapacciuolo, G. Polito, V. Bisesti, F. Manguso, et al. 2006. Combined use of noninvasive tests is useful in the initial diagnostic approach to a child with suspected inflammatory bowel disease. *J. Pediatr. Gastroenterol. Nutr.* 42: 9–15.
72. Costa, F., M. G. Mumolo, L. Ceccarelli, M. Bellini, M. R. Romano, C. Sterpi, A. Ricchiuti, S. Marchi, and M. Bottai. 2005. Calprotectin is a stronger predictive marker of relapse in ulcerative colitis than in Crohn's disease. *Gut* 54: 364–368.
73. Däbritz, J., F. Friedrichs, T. Weinhage, J. Hampe, T. Kucharzik, A. Lügering, U. Broeckel, S. Schreiber, T. Spieker, M. Stoll, and D. Foell. 2011. The functional -374T/A polymorphism of the receptor for advanced glycation end products may modulate Crohn's disease. *Am. J. Physiol. Gastrointest. Liver Physiol.* 300: G823–G832.
74. Sims, G. P., D. C. Rowe, S. T. Rietdijk, R. Herbst, and A. J. Coyle. 2010. HMGB1 and RAGE in inflammation and cancer. *Annu. Rev. Immunol.* 28: 367–388.
75. Lee, M. J., J. K. Lee, J. W. Choi, C. S. Lee, J. H. Sim, C. H. Cho, K. H. Lee, I. H. Cho, M. H. Chung, H. R. Kim, and S. K. Ye. 2012. Interleukin-6 induces S100A9 expression in colonic epithelial cells through STAT3 activation in experimental ulcerative colitis. *PLoS ONE* 7: e38801.